# Photoluminescence in Analysis of Surfaces and Interfaces

*Timothy H. Gfroerer*

in
*Encyclopedia of Analytical Chemistry*
R.A. Meyers (Ed.)
pp. 9209–9231
© John Wiley & Sons Ltd, Chichester, 2000

# Photoluminescence in Analysis of Surfaces and Interfaces

**Timothy H. Gfroerer**
*Davidson College, Davidson, USA*


**1 Introduction** 1
**2 Photoluminescence Excitation** 3
2.1 Excitation Energy: Penetration Depth and Stoke's Shift 3
2.2 Excitation Intensity: Interface State Density and Distribution 4
**3 Photoluminescence Spectrum** 7
3.1 Photoluminescence Peak Positions: Energy Levels 8
3.2 Photoluminescence Line Width and Splitting: Alloy Disorder and Interface Roughness 10
**4 Photoluminescence Intensity** 12
4.1 Dependence on Applied Bias: Surface Potential 13
4.2 Spatial Dependence: Interface Uniformity and Carrier Diffusion 14
4.3 Time Dependence: Recombination Rates 16
4.4 Temperature Dependence: Thermal Population 18
**5 Photoluminescence Polarization** 19
**6 Conclusion** 20
**Abbreviations and Acronyms** 20
**Related Articles** 21
**References** 21


*Photoluminescence (PL) is the spontaneous emission of light from a material under optical excitation. The excitation energy and intensity are chosen to probe different regions and excitation concentrations in the sample. PL investigations can be used to characterize a variety of material parameters. PL spectroscopy provides electrical (as opposed to mechanical) characterization, and it is a selective and extremely sensitive probe of discrete electronic states. Features of the emission spectrum can be used to identify surface, interface, and impurity levels and to gauge alloy disorder and interface roughness. The intensity of the PL signal provides information on the quality of surfaces and interfaces. Under pulsed excitation, the transient PL intensity yields the lifetime of nonequilibrium interface and bulk states. Variation of the PL intensity under an applied bias can be used to map the electric field at the surface of a sample. In addition, thermally activated processes cause changes in PL intensity with temperature.*

*PL analysis is nondestructive. Indeed, the technique requires very little sample manipulation or environmental control. Because the sample is excited optically, electrical contacts and junctions are unnecessary and high-resistivity materials pose no practical difficulty. In addition, time-resolved PL can be very fast, making it useful for characterizing the most rapid processes in a material. The fundamental limitation of PL analysis is its reliance on radiative events. Materials with poor radiative efficiency, such as low-quality indirect bandgap semiconductors, are difficult to study via ordinary PL. Similarly, identification of impurity and defect states depends on their optical activity. Although PL is a very sensitive probe of radiative levels, one must rely on secondary evidence to study states that couple weakly with light.*

## 1 INTRODUCTION

Multilayer material systems are increasingly important in the development of smaller, faster, and more efficient electronic and optoelectronic devices. The primary motivation for using multilayer structures is to change the potential energy of electrons and holes at the material interfaces. Because phenomena at surfaces and interfaces tend to dominate the behavior of excitations in these heterostructures, the performance of many microelectronic devices is limited by the nature of heterojunctions. Smooth and atomically abrupt interfaces are necessary for good optical and electrical reflection, uniform quantum confinement, and high carrier mobility. Even more importantly, defects and impurities at interfaces provide new states for electrons and holes, altering their motion, lifetime, and transition energies.

When light of sufficient energy is incident on a material, photons are absorbed and electronic excitations are created. Eventually, these excitations relax and the electrons return to the ground state. If radiative relaxation occurs, the emitted light is called PL. This light can be collected and analyzed to yield a wealth of information about the photoexcited material. The PL spectrum provides the transition energies, which can be used to determine electronic energy levels. The PL intensity gives a measure of the relative rates of radiative and nonradiative recombination. Variation of the PL intensity with external parameters like temperature and applied voltage can be used to characterize further the underlying electronic states and bands.

*Encyclopedia of Analytical Chemistry*
R.A. Meyers (Ed.) Copyright © John Wiley & Sons Ltd

PL depends on the nature of the optical excitation. The excitation energy selects the initial photoexcited state and governs the penetration depth of the incident light. The PL signal often depends on the density of photoexcited electrons, and the intensity of the incident beam can be adjusted to control this parameter. When the type or quality of material under investigation varies spatially, the PL signal will change with excitation position. In addition, pulsed optical excitation provides a powerful means for studying transient phenomena. Short laser pulses produce virtually instantaneous excited populations, after which the PL signal can be monitored to determine recombination rates.

Because PL often originates near the surface of a material, PL analysis is an important tool in the characterization of surfaces. The utility of PL for this purpose is derived from its unique sensitivity to discrete electronic states, many of which lie near surfaces and interfaces. Using the techniques noted above, the nature of these states can be probed in detail. The energy distribution and density of interface states can be ascertained by studying the excitation intensity dependence of the PL spectrum. The presence of surface adsorbates alters the intensity of the PL signal. When the states serve as long-lived traps, the depth of the trap can be determined by observing thermal activation in temperature-dependent PL. In fact, even if interface states are nonradiative, which is usually the case, the states alter the time-resolved PL of radiative transitions in the material. Nonradiative traps dominate the transient PL signal at low carrier density.

PL is simple, versatile, and nondestructive. The instrumentation that is required for ordinary PL work is modest: an optical source and an optical power meter or spectrophotometer. A typical PL set-up is shown in Figure 1. Because the measurement does not rely on electrical excitation or detection, sample preparation is minimal. This feature makes PL particularly attractive for material systems having poor conductivity or undeveloped contact/junction technology. Measuring the continuous wave PL intensity and spectrum is quick and straightforward. On the other hand, investigating transient PL is more challenging, especially if recombination processes are fast. Instrumentation for time-resolved detection, such as single photon counting, can be expensive and complex. Even so, PL is one of the only techniques available for studying fast transient behavior in materials.

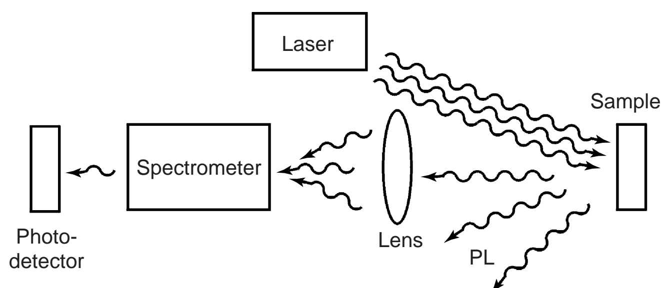


**Figure 1** Typical experimental set-up for PL measurements.

Because PL can be used to study virtually any surface in any environment, it can be used to monitor changes induced by surface modification in real time. For example, unlike most surface characterization techniques, PL is generally not sensitive to the pressure in the sample chamber. Hence, it can be used to study surface properties in relatively high-pressure semiconductor growth reactors. Although PL does depend quite strongly on temperature, liquid helium temperatures being required for the highest spectral resolution, room-temperature measurements are sufficient for many purposes. In addition, PL has little effect on the surface under investigation. Photoinduced changes and sample heating are possible, but low excitation can minimize these effects. In situ PL measurements do require optical access to the sample chamber. Yet, compared with other optical methods of characterization like reflection and absorption, PL is less stringent about beam alignment, surface flatness, and sample thickness.

The advantages of PL analysis listed above derive from the simplicity of optical measurements and the power to probe fundamental electronic properties. The chief drawback of PL analysis also follows from the reliance on optical techniques: the sample under investigation must emit light. Indirect-bandgap semiconductors, where the conduction band minimum is separated from the valence band maximum in momentum space, have inherently low PL efficiency. Nonradiative recombination tends to dominate the relaxation of excited populations in these materials. This problem can be augmented by poor surface quality, where rapid nonradiative events may occur. Nevertheless, once a PL signal is detected, it can be used to characterize both radiative and nonradiative mechanisms. Although it may not be possible to identify directly the nonradiative traps via PL, their signature is evident in several types of PL measurements.

Another shortcoming of PL is the difficulty in estimating the density of interface and impurity states. When these states have radiative levels, they are readily identified in the PL spectrum, and the size of the associated PL peaks provides a relative measure of their presence in the sample. However, measuring the absolute density of these states is a far more formidable task and typically requires an exhaustive analysis of the excitation intensity dependence of the PL signal.

## 2 PHOTOLUMINESCENCE EXCITATION

The choice of excitation is critical in any PL measurement. The excitation energy and intensity will have profound effects on the PL signal. Although the excitation conditions must be considered carefully, the strength of the PL technique relies heavily on the flexibility that these adjustable parameters provide. Because the absorption of most materials depends on energy, the penetration depth of the incident light will depend on the excitation wavelength. Hence, different excitation energies probe different regions of the sample. The excitation energy also selects the initial excited state in the experiment. Because lasers are monochromatic, intense, and readily focused, they are the instruments of choice for photoluminescence excitation (PLE). For many applications, the excitation energy is not critical. Here, a relatively inexpensive HeNe or diode laser will often satisfy the basic requirement of light exceeding the bandgap energy. In more demanding experiments, the laser is chosen carefully to probe a particular depth or to excite a particular species in the sample.

Unlike the excitation energy, which may or may not be important, the excitation intensity will influence the result of any PL experiment. The excitation intensity controls the density of photoexcited electrons and holes, which governs the behavior of these carriers. Each electron–hole recombination mechanism has a distinct functional dependence on carrier density. For example, the number of interface and impurity states is finite, and recombination at these sites will saturate at high excitation. In addition, the photoexcited carriers themselves can alter the distribution of interface states. Thus, the excitation intensity must be calibrated accurately and controlled precisely.

### 2.1 Excitation Energy: Penetration Depth and Stoke's Shift

The absorption of a material depends strongly on the energy of the incident light. In the analysis of surfaces, it is useful to describe this wavelength-dependent absorption by a penetration depth (the inverse of the absorption coefficient), which is a measure of the thickness of the layer that is probed. In direct-bandgap semiconductors, above-bandgap excitation has a penetration depth of the order of 1 µm. The diffusion of photoexcited carriers can vary widely but is typically in the range 1–10 µm. Hence, PL with above-gap excitation is very sensitive to surface effects. In indirect-bandgap semiconductors, or direct-gap semiconductors with sub-bandgap excitation, absorption is weaker and the light penetrates deeper into the sample. Here, the PL is dominated by bulk recombination. If multiple excitation wavelengths are available, this property of PL can be used to distinguish surface and bulk contributions.

Garcia-Garcia et al. have used such an approach to study the surface layer of chemically etched CdTe.[1] When the surface structure is poor, the PL spectrum changes with increasing excitation energy, the strength of defect-related lines increasing relative to bulk features. Correlation of these changes with penetration depth indicates the location of near-surface defects. Furthermore, the authors found that the PL spectrum of a high-quality surface is independent of excitation energy. In an extension of this technique, Wang et al. used the widely divergent penetration of one and two photon absorption processes to distinguish surface and bulk effects.[2] In contrast to relatively slow recombination with two-photon excitation, a fast recombination mechanism dominated the one-photon excitation experiment. This result indicates the presence of rapid recombination sites near the surface of the semiconductor, where the single-photon excitation is absorbed.

Dangling bonds at a semiconductor surface or interface give rise to electronic states within the bandgap. These mid-gap states fill up to the Fermi level with electrons that originate in the bulk of the material. The accumulation of charge at the surface creates an electric field – a depletion region – that leads to bending of the valence and conduction band edges. According to a simple dead-layer model,[3] electron–hole pairs that are generated in this region are swept apart by the electric field, prohibiting radiative recombination. The phenomenon is described quantitatively by a depletion thickness that characterizes this "dead layer".

Although the dead-layer picture of carrier kinetics at the surface of a semiconductor overlooks the complicated role of surface states in the recombination process, it is useful when PL quenching has an electrostatic origin. For example, Ryswyk and Ellis have studied the effect of $I_2$ on n-GaAs in the context of this model.[4] They used PL depth profiling with multiple excitation wavelengths to determine the depletion thickness in the $I_2$-treated sample. Uosaki et al.[5] have used a similar experimental approach to characterize p-GaAs/electrolyte interfaces. Results were analyzed within the context of the more sophisticated model proposed by Mettler,[6] which accounts for changes in charge separation *and* surface state recombination. It should be noted that these phenomena are intricately connected, and resolving their contributions to PL quenching is difficult. Although changes in the electric field at the surface should not affect the surface state density, altering the nature or number of surface states can affect depletion and band bending. This point will be discussed in more detail in section 4.

In addition to controlling the penetration depth, the excitation energy selects the initial photoexcited state in the sample. This state is short-lived because thermalization of photoexcited carriers via phonon emission is rapid. Relaxation to within $kT$ of the lowest available states is usually orders of magnitude faster than recombination. Thus, ordinary PL emission only reveals the lowest energy states. Nevertheless, it is possible to obtain spectral information on excited states by collecting the low-energy emission while tuning the excitation energy across higher energy states. The PL signal is enhanced when the excitation energy is resonant with an excited state. The technique, called photoluminescence excitation spectroscopy, is similar to ordinary absorption subject to the condition that there exists a relaxation channel from the excited state to the emission state being monitored. PLE is frequently used to study epilayers on opaque substrates because absorption is not feasible in this case.

Compared to band continua, discrete interface states are relatively sparse. PL is easily dominated by interface states because such states tend to have levels below the intrinsic bands, and carriers are remarkably efficient at finding the lowest available states. However, PLE relies on optical absorption, which is relatively weak for isolated interface sites. Hence, it is usually difficult to uncover interface states in PLE spectra. Nevertheless, PLE has been applied successfully to the characterization of certain surface species. For example, Zhu et al. utilized PLE to identify groups chemisorbed on the surface of $TiO_2$ ultrafine particles.(7) Similarly, Anpo et al. used the dependence of PL on excitation energy to resolve differences between anchored and impregnated $Mo/SiO_2$ catalysts.(8)

An important feature of optical transitions in semiconductor quantum wells (QWs) is the energy difference between the absorption (or PLE) and emission peaks – Stoke's shift. This shift is a measure of interface fluctuations because it indicates that the thickness of the QW varies with position. Carriers are photoexcited uniformly in the QW but they diffuse to regions of larger well width, where the confinement energy is smaller, before recombining. Deveaud et al. have studied the PL and PLE spectra of a series of multiple QW samples.(9) In samples prepared under optimal growth conditions, they observed two sharp PL peaks, which they attribute to recombination in regions where the QW thickness differs by exactly one atomic monolayer. PLE is used to test whether excitation at the higher energy peak yields emission from the lower energy peak and to confirm that thermalization between the two regions occurs. It has been argued that splittings in PL from QWs like those discussed above can be misleading because impurities can produce similar effects.(10) The ambiguity can be resolved by using PLE where impurity transitions are weak. The structure in PL spectra from QWs will be discussed in more detail in section 3.2.

### 2.2 Excitation Intensity: Interface State Density and Distribution

The intensity of the incident light controls a critical property of the PL experiment: the density of photoexcited electrons and holes. When the carrier density is low, the measurement is dominated by discrete defect and impurity sites at the interfaces and within the bulk of the material. Recombination at these energetically favored sites is frequently referred to as Shockley–Read–Hall (SRH) recombination, in recognition of early work on the statistics of this phenomenon. The SRH rate is proportional to the dominant carrier density $n$. The dominant carrier density is the greater of two quantities: the equilibrium carrier concentration (i.e. the doping level) and the photoexcited carrier concentration. Under intermediate excitation, the discrete states are filled and bulk radiative recombination plays a greater role. Neglecting excitonic effects, these transitions are two-body events between free electrons and holes, so the radiative rate varies as $n^2$. It should be noted that low temperatures or quantum confinement can make Coulomb binding of electron–hole pairs energetically favorable, leading to the formation of excitons that recombine radiatively at a rate proportional to $n$. At the highest carrier densities, three-body Auger recombination becomes important because the rate of this mechanism varies as $n^3$. In the analysis of interfaces, the transition between SRH and radiative recombination is the most important because it depends on the density of defect and impurity sites.

In systems with high interface-to-volume ratios and active layers that are thin relative to the carrier diffusion length, interface effects dominate SRH recombination. In planar structures, the interface-to-volume dependence of SRH recombination can be separated from actual interface phenomena via the interface recombination velocity $S$. The interface recombination rate is defined as $R_s = (S/d)n$, where $d$ is the thickness of the optically active layer. When two interfaces are present, as in a double heterostructure, the two interface contributions are combined: $S$ is replaced by $S_1 + S_2$ (or $2S$ for equivalent interfaces). Because $S$ is independent of carrier density and layer thickness, it can be used to compare interface recombination in a variety of materials. $S$ depends strongly on the nature of the interface. For example, $S$ is of the order of $10^7\,cm\,s^{-1}$ at the interface of GaAs and air, whereas high-quality GaAs/GaInP interfaces can have $S < 10\,cm\,s^{-1}$.(11)

This reduction of the interface recombination velocity at the edge of a material is called surface passivation.

Because the performance of many optoelectronic devices is limited by interface recombination, interface passivation has been studied extensively. Passivation techniques include epitaxial growth of lattice-matched semiconductor alloys and a variety of chemical surface treatments. Qualitative evaluation of these techniques is straightforward: an increase in the PL signal indicates a decrease in nonradiative interface recombination. Quantitative information on $S$ requires more sophisticated techniques, many of which involve investigations of the excitation intensity dependence of PL.

Komiya et al. measured the excitation-intensity-dependent PL signal from a series of InGaAsP/InP double heterostructures.(12) Although the PL signal was usually linear with excitation power, some samples showed superlinear dependence under intermediate excitation (see Figure 2), indicating a transition between nonradiative and radiative recombination regimes. The lack of such a transition in the other samples suggests that radiative recombination dominated at all excitation levels, which gave an upper limit for $S$. In a very different approach, Mullenborn and Haegel studied single AlGaAs/GaAs and GaInP/GaAs heterostructures where the buried GaAs layer is excited indirectly via either carrier diffusion or recycling (i.e. reabsorption and emission) of photons.(13) The excitation intensity dependence of PL from both layers was used to distinguish between the two mechanisms for carrier generation in the buried layer. Because

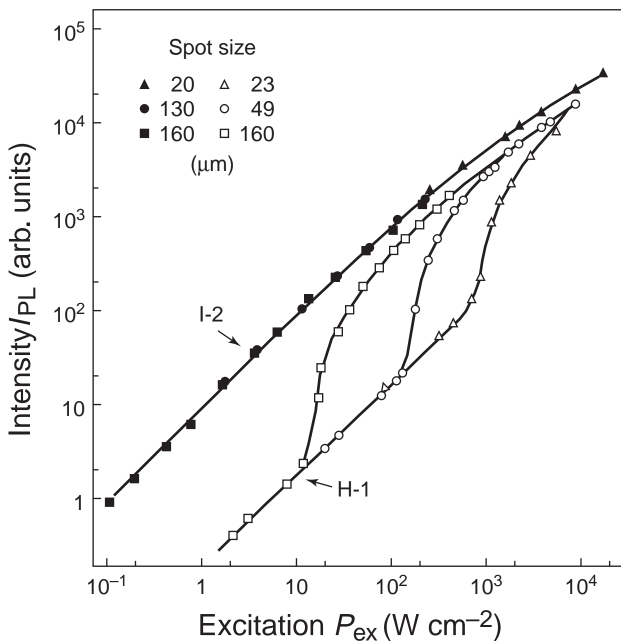


**Figure 2** Excitation power dependence of the PL intensity for two different samples. The I-2 PL signal is approximately linear with excitation, whereas the H-1 signal increases superlinearly in the intermediate excitation regime.(12)

the two processes are competing, and react differently to interface quality, their relative strengths can be modeled to characterize interface recombination.

The experiments described above combine relative measurements of the PL intensity with considerable assumptions or modeling to obtain quantitative information on semiconductor interfaces. Absolute measurements of the PL intensity provide for a more direct analysis of interfaces. Evaluating the absolute PL intensity requires an estimate of what fraction of the emitted light is collected by the detector. However, the PL emission profile is a complicated function of sample geometry, refraction, internal reflection, and reabsorption. Hence, large uncertainties in this estimate are inevitable. Integrating spheres can be used to ensure that most of the emission is collected, but it is difficult to control environmental parameters such as temperature in these devices.

A very accurate alternative technique for measuring the absolute PL intensity from light-emitting materials with unspecified emission profiles has been developed.(14) The sample can be studied in a controlled environment, and the measurement does not require knowledge of the fraction of emission collected. Determination of the absolute PL intensity relies on the fact that simultaneous relative measurements of radiative and nonradiative recombination can be combined to determine the absolute radiative efficiency (the ratio of photons emitted to photons absorbed). Because the excitation power must be converted into either light or heat, an increase in one must be accompanied by a proportional decrease in the other. The intensity of the emitted light and the temperature change are measured as a function of excitation power to evaluate the relative strength of the radiative and nonradiative mechanisms. Then, extrapolating the temperature change to zero heating, the light signal equivalent to 100% radiative efficiency is obtained.

This technique has been used to measure the absolute radiative efficiency of an InGaAs/InP double heterostructure with an integral substrate reflector.(14) A plot of the normalized light signal vs. temperature change is shown in Figure 3. At low excitation, the relative intensity of the emitted light increases, and the relative temperature change decreases with increasing excitation. However, at high excitation the radiative efficiency rolls off (see Figure 4), and the data begin to show the opposite trend. As predicted by the model described above, the points fall on a straight line and do not depend on whether the efficiency is increasing or decreasing with excitation. Extrapolation to zero heat is not shown in Figure 3 because a false origin is required to give sufficient detail. Nevertheless, the $y$-intercept of the linear fit in Figure 3 can be combined with the excitation and average emission energies to calibrate the relative light signal data. The result of this calibration is presented in Figure 4.

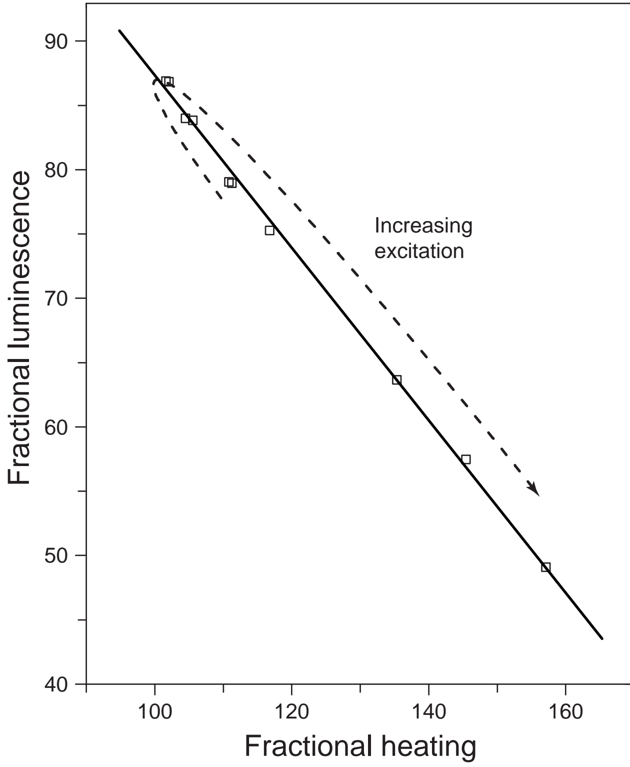


**Figure 3** Relative measurements of luminescence signal and temperature change, normalized by the excitation intensity and plotted against each other. The dotted line indicates how the result evolves as the excitation power is increased.[14]

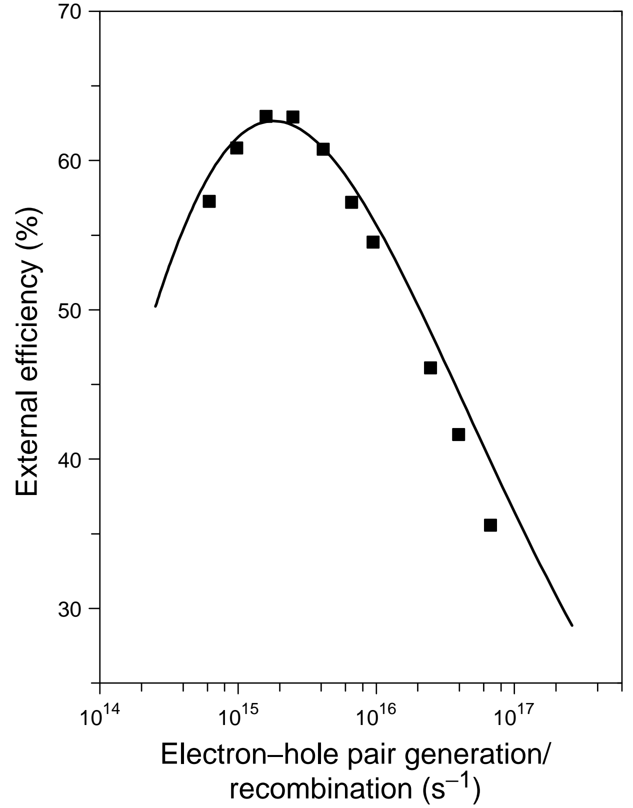


**Figure 4** External radiative quantum efficiency vs. the rate of electron–hole pair generation and recombination in steady state. The solid line is a fit to the data that accounts for interface, radiative, and Auger recombination events.[14]

The fit in Figure 4 relies on the fact that, in steady state, the rate of carrier generation equals the rate of recombination, as shown in Equation (1):

$$\frac{P_{\mathrm{abs}}}{E_{\mathrm{ex}}} = V\left(\frac{2S}{d}n + \frac{B}{N}n^2 + Cn^3\right) \tag{1}$$

Here, $P_{\mathrm{abs}}$ is the absorbed laser power, $E_{\mathrm{ex}}$ is the laser energy, and $V$ is the volume. The photon recycling factor $N$ is the average number of radiative recombination events required for a photon to escape the semiconductor, and $B$ and $C$ are parameters that describe the rates of radiative and Auger recombination respectively. Because the fit is very sensitive to the coefficients that characterize the different mechanisms for recombination, it can be used to evaluate parameters such as the interface recombination velocity $S$.

Saitoh et al. have argued that the simple picture of an excitation-independent surface recombination velocity is not sufficient to describe the excitation dependence of the PL signal.[15] In particular, when the excitation is intermediate between the SRH and radiative recombination-dominated regimes, the quasi-Fermi levels for electrons and holes split away from the low-excitation pinned position and move toward their respective band edges. The quasi-Fermi levels determine the energy range of surface states that contribute to recombination. Thus, the PL efficiency in this transition region is very sensitive to the density and energy distribution of surface states. The authors have developed an elaborate model of carrier behavior near the surface of the semiconductor that accounts for carrier transport, surface state occupation, band bending, and recombination. Analysis of the excitation-intensity-dependent PL signal in the context of this model is referred to as photoluminescence surface-state spectroscopy (PLS$^3$).

The shape of the radiative efficiency curve in the SRH to radiative recombination transition region depends on the distribution of surface states that participate in recombination. If the distribution consists of a discrete set of states with similar energetic positions within the gap, complete saturation of the SRH recombination process will lead to a PL efficiency slope of unity. Efficiency curves with slopes less than unity indicate that the surface-state distribution is continuous and that an increasing number of surface states are participating in recombination as the quasi-Fermi levels move through the bandgap. Hence, variation in the slope of the efficiency curve with

increasing excitation can be used to map the surface-state distribution within the gap. Two distinct surface-state distributions and their corresponding efficiency curves are shown in Figure 5.[16] Since its development in 1991, $PLS^3$ has been applied to a wide number of semiconductor systems. Although some of these studies have uncovered surface states with discrete energies, most have revealed that the surface-state distribution is U-shaped, with increasing density near the band edges.

Excitation-intensity-dependent PL can also be used to study the properties of QWs. Ding et al. measured the excitation intensity $I_{ex}$ dependence of the integrated PL signal from asymmetric coupled QWs.[17] They note that the PL intensity should vary as $I_{ex}^2$ when recombination is dominated by nearly saturated interface traps, but should be proportional to $I_{ex}$ when radiative recombination is more important. This behavior was clearly observed in their results. They used the transition intensity to estimate the nonradiative decay time, which suggested that traps were located at the interface of the coupling barrier and the larger well. Excitation-dependent saturation of PL can also be used to determine the relative density of different radiative states. For example, when splittings are observed in the PL from QWs, as described in section 2.1, the lower energy peak often saturates with increasing excitation because of state filling. In this case, the saturation intensity can be used to estimate the size of interface islands in the QW where the lower energy PL is believed to originate.[18]

A third application of excitation-intensity-dependent PL is in the evaluation of interface band alignment. Vignaud et al. observed a dramatic excitation-dependent blueshift in the PL from InAlAs/InP heterostructures. They attributed this blueshift to spatially indirect type II transitions across the interface.[19] The blueshift is explained as follows: when the conduction band minimum and valence band maximum occur on opposite sides of a semiconductor interface, electrons and holes are trapped in different regions of the heterostructure. Because the electrons and holes are attracted to each other, narrow QWs are formed adjacent to the interface, as shown in Figure 6. As the excitation is increased, carriers accumulate in these wells, increasing the confinement energy of the wells and the dipole energy across the interface. Both of these mechanisms lead to substantial blueshifts in the PL. It is interesting to note that type II transitions, which occur across the interface itself, are especially sensitive to interface quality.

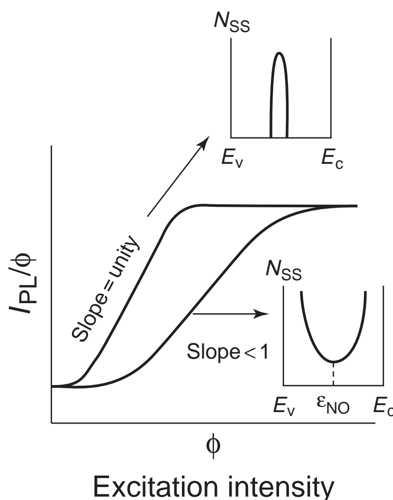


**Figure 5** Relative PL efficiency $I_{PL}/\Phi$ vs. excitation intensity $\Phi$ for discrete and U-shaped surface-state distributions.[16]

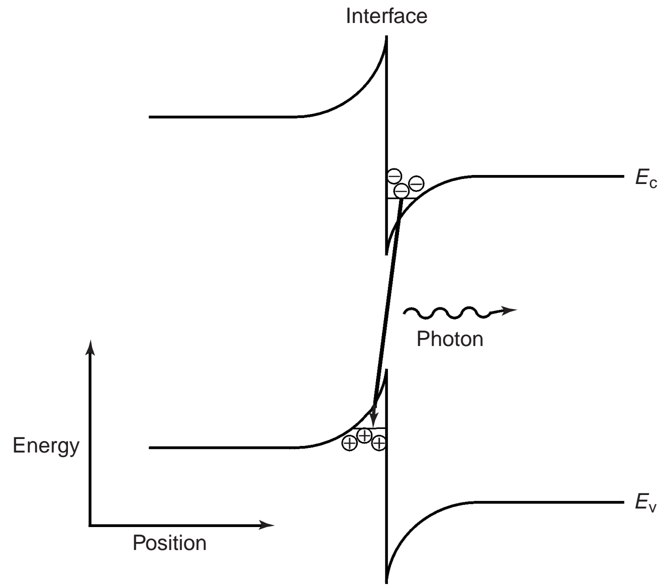


**Figure 6** Type II band alignment where electrons and holes collect on opposite sides of a semiconductor interface. The small QWs that form near the interface lead to a substantial excitation-dependent blueshift in the PL.

## 3 PHOTOLUMINESCENCE SPECTRUM

Optical transitions provide direct access to the energy level structure of a system. Photons of a particular energy that are absorbed or emitted by a sample provide evidence of electronic states differing by that energy within the material. Absorption is a good probe of the overall band structure of a system because bands have a relatively high density of states. PL emission, on the other hand, tends to favor sparse low-lying states because photoexcited carriers rapidly thermalize through bands and closely spaced states to within $kT$ of the lowest available levels. This feature of PL makes it particularly effective in the analysis of interfaces where discrete defect and impurity states

abound. If the state is radiative, it will generate unique peaks in the PL spectrum. Thus, the PL measurement is a very sensitive and selective probe of such states.

In addition to identifying discrete states, PL peak positions can be used to evaluate the composition of semiconductor alloys. Here, the energy of the band-edge emission is correlated with the composition-dependent bandgap of the alloy. This application is also useful in interface analysis where atomic interdiffusion leads to interface alloying. Interface alloys can form narrow wells or barriers that have an impact on the behavior of carriers at heterojunctions. Evidence of interface wells and barriers is often found in the PL spectrum.

Other features of the PL spectrum, including line widths and splittings, provide important information on QW interfaces. These systems are very sensitive to interface roughness because fluctuations as small as one atomic monolayer can alter the carrier confinement energy considerably. When the QW thickness varies substantially within the sampled region, a general broadening of the PL spectrum is observed. In samples with higher quality interfaces, variation in the QW thickness is limited, and recombination in different regions yields sharp, well-resolved peaks in the PL.

### 3.1 Photoluminescence Peak Positions: Energy Levels

In the bulk of a crystalline material, translational symmetry leads to the formation of electronic energy bands. Defects and impurities break the periodicity of the lattice and perturb the band structure locally. The perturbation usually can be characterized by a discrete energy level that lies within the bandgap. Depending on the defect or impurity, the state acts as a donor or acceptor of excess electrons in the crystal. Electrons or holes are attracted to the excess or deficiency of local charge due to the impurity nucleus or defect, and Coulomb binding occurs. The situation can be modeled as a hydrogenic system where the binding energy is reduced by the dielectric constant of the material. Because electrons and holes have different effective masses, donors and acceptors have different binding energies.

When the temperature is sufficiently low, carriers will be trapped at these states. If these carriers recombine radiatively, the energy of the emitted light can be analyzed to determine the energy of the defect or impurity level. Shallow levels, which lie near the conduction or valence band edge, are more likely to participate in radiative recombination, but the sample temperature must be small enough to discourage thermal activation of carriers out of the traps. Deep levels tend to facilitate nonradiative recombination by providing a stop-over for electrons making their way between the conduction and valence bands by emitting phonons. Several intrinsic and impurity transitions are illustrated in Figure 7.

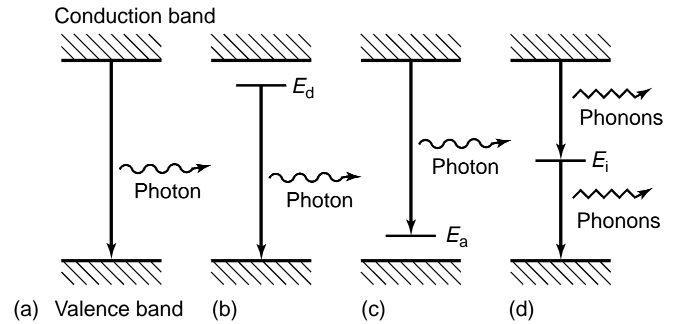


**Figure 7** (a–c) Radiative recombination paths: (a) band-to-band; (b) donor to valence band; (c) conduction band to acceptor. (d) Nonradiative recombination via an intermediate state.

Surfaces and interfaces usually contain a high concentration of impurity and defect states. As the physical termination of the sample, the surface represents a drastic interruption of the material itself. Dangling bonds often provide numerous midgap states that facilitate rapid nonradiative recombination. They also act as getters for ambient impurities. Dangling bonds can be accommodated by a variety of surface treatments and lattice-matching semiconductor epilayers. Even so, impurities accumulate on surfaces before treatment and during growth interruptions. In addition, interface defects due to slight lattice mismatch at semiconductor heterojunctions are inevitable.

In systems where the interfaces and bulk material contribute to the PL, the two components can be distinguished via depth profiling. Thewalt et al. combined PL with spreading resistance analysis (SRA) depth profiling to identify the type and location of several impurities in ultrahigh-purity epitaxial silicon.[20] PL spectra of the substrate and three epitaxial samples are shown in Figure 8. The strong Al line in sample (c) and the weaker line in sample (b) correlate well with an interfacial contaminant detected in SRA. Destructive depth profiling can be accomplished by step-etching and measuring the PL vs. etch depth. Akimoto et al. used this approach to connect specific PL peaks with vacancy complexes at a GaAs/AlGaAs interface.[21]

Some good examples of PL spectral analysis in the characterization of bare surfaces are in the field of semiconductor etching. Reactive ion etching (RIE), where etching is accomplished by bombarding the surface with energetic reactive ions, is an important procedure in the fabrication of optoelectronic devices with submicron features. However, RIE can produce various types of defects in the near-surface region. For optimal device performance, the damage and contamination caused by

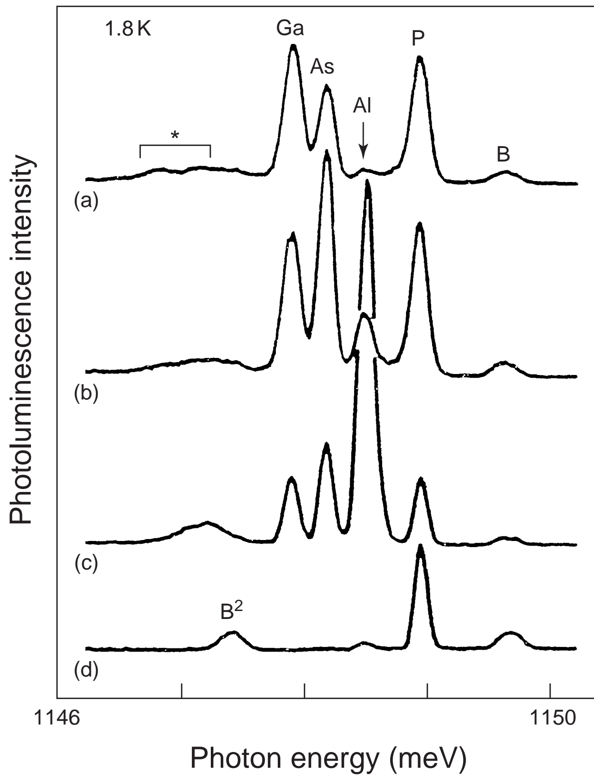


**Figure 8** PL spectra of three epitaxial Si samples (a–c) and the substrate material (d) showing spectral lines associated with Ga, As, Al, P, and B impurities.[20]

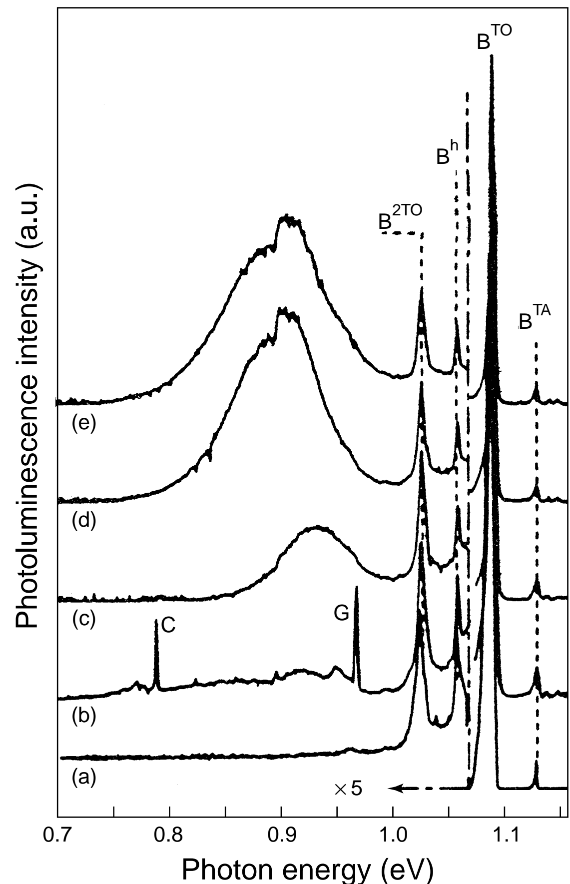


**Figure 9** PL spectra of B-doped Si after the following plasma exposures: (a) 80% He–20% HBr; (b) $CF_4$; (c) Ar; (d) Ar-$D_2$; (e) $D_2$.[22]

RIE should be minimized. PL analysis is very useful in identifying and controlling RIE-induced defects.

Henry et al. used PL to study the effects of various plasmas on exposed surfaces of phosphorus- and boron-doped silicon.[22] As shown in Figure 9, the PL spectrum depended strongly on the plasma composition. Before treatment, the spectrum consisted of a number of lines just below the bandgap that are associated with the boron dopant in the material ($B^{TA}$, $B^{TO}$, $B^{h}$, and $B^{2TO}$). No deep luminescence was observed in the control sample. After treatment, several deep luminescence features emerged in the PL spectrum. The features can be divided into two categories: sharp lines and broad bands. The sharp lines are characteristic of radiative transitions at deep neutral defects in silicon, which are known from other studies involving high-energy particle irradiation. For example, the lines labeled C and G in spectrum 9(b) are recognized as transitions associated with carbon-related defects in silicon. The origin of the broad bands observed in spectra 9(c–e) is not completely understood. It is attributed to recombination at extended defects where the strained silicon lattice creates local potential wells that trap electrons and holes.

Broad, deep PL emission is a common characteristic of damaged semiconductors. Foad et al. have investigated changes in the PL spectrum of ZnTe/GaAs epitaxial layers after RIE and subsequent annealing.[23] RIE leads to a factor of 100 reduction in the near-band-edge emission, accompanied by the appearance of very broad new features well below the gap. One of the low-energy peaks coincides with a specific defect found in bulk ZnTe, but the peak is much broader than observed previously. Upon annealing, near-band-edge PL recovers by one order of magnitude and the deep emission shows more structure, revealing that the very broad, deep emission seen prior to annealing was actually composed of several phonon replicas (transitions assisted by one or more phonons). The annealing results suggest that the strain around RIE-induced defects is reduced.

Deep emission has also been attributed to dislocation networks at the interface of lattice-mismatched heterostructures. The effects of strain and dislocations can be separated in InGaAs/GaAs heterostructures where accommodation of lattice mismatch depends on the InGaAs layer thickness. Strain dominates when the InGaAs is thin, but the strain is relaxed by the formation

of misfit dislocations when the InGaAs layer exceeds a critical thickness. Joyce et al. observed broad, deep PL in the InGaAs/GaAs system and measured the spectrum as a function of InGaAs thickness.[24] They found that the intensity of the deep emission increases rapidly above the critical thickness, suggesting that interface dislocations are responsible for the broad, sub-bandgap PL.

As with surface damage, relative changes in surface state and band-edge emission can be used to evaluate surface passivation. For example, Xu et al. have used PL to study the properties of CuSe coatings on CdSe nanocrystals.[25] The uncoated CdSe nanocrystals produced broad, sub-bandgap PL, which they attributed to recombination at deep surface traps. With increasing CuSe fraction on the CdSe cores, they observed a monotonic decrease in this emission accompanied by steadily increasing band-edge PL. Ordinarily, materials with larger bandgaps are required for surface passivation so that carriers see potential barriers at the interface, shielding them from the surface. Because CuSe has a smaller bandgap than CdSe, surface passivation with this material is unusual. The authors suggest that the CuSe coating is very thin so that the CuSe gap is enhanced by quantum confinement.

Although spectral analysis of sub-bandgap emission is useful for characterizing interfaces, the peak position of the band-edge PL itself provides important information on atomic interdiffusion and interface alloying. The bandgap of a semiconductor alloy depends directly on alloy composition. When heterojunctions are not abrupt, unintentional alloy layers are formed at the interface. Depending on composition, such layers can have bandgaps larger, smaller, or intermediate between the adjoining materials. For example, Guimaraes et al. observed an anomalous emission band below the GaAs and GaInP gaps in GaInP/GaAs heterostructures.[26] They postulated that the band was due to recombination in GaInPAs intermediate layers, and confirmed their hypothesis by observing an enhancement of the band with an As-rich growth interruption at the interface.

Exchange or accumulation of atomic species at interfaces has a drastic impact on recombination in semiconductor QWs where individual monolayers of material are significant. GaInP/GaAs QW energies reported in the literature vary by as much as 100 meV for well widths below 10 monolayers. Mesrine et al. have shown that this scatter can be explained by two growth-related mechanisms: As/P exchange at interfaces and In surface segregation on GaInP layers.[27] Limiting cases incorporating a single monolayer of InAs or GaP at an interface more than account for the dispersion in PL energies obtained by different groups.

### 3.2 Photoluminescence Line Width and Splitting: Alloy Disorder and Interface Roughness

Whereas graded interfaces are likely to shift transition energies, interface roughness tends to produce line broadening and splitting in QWs. QW PL peaks are almost always broader than bulk PL. The line broadening is attributed to unintentional variation in the confinement energy in different regions of the well. Two distinct mechanisms contribute to lateral variation in the QW properties: alloy disorder in the well or barrier layers, and interface roughness. When the line width increases rapidly with decreasing well width $L$, the broadening is usually attributed to interface roughness. The confinement energy depends heavily on $L$ in narrow wells and, assuming that the scale of interface fluctuations does not depend on layer thickness, decreasing the well width means that the fractional variation in $L$ is larger. Alloy disorder can also lead to well-width-dependent PL broadening, especially when the disorder is concentrated in the barrier layers. In this case, reducing the well width causes the wavefunction of confined carriers to penetrate deeper into the barriers, thus sampling increasing amounts of disorder.

When optimal growth conditions are achieved, interface fluctuations can be restricted to a single monolayer of atoms and the average lateral extent of atomically smooth interfaces is larger than the wavefunction of the confined state. When PL measurements are conducted at liquid helium temperatures, the confined states are usually Coulomb-bound electron–hole pairs, or excitons. Several possible scenarios for excitons in QWs with single-monolayer fluctuations are shown in Figure 10. Typically, the lateral extent of atomically smooth islands is smaller

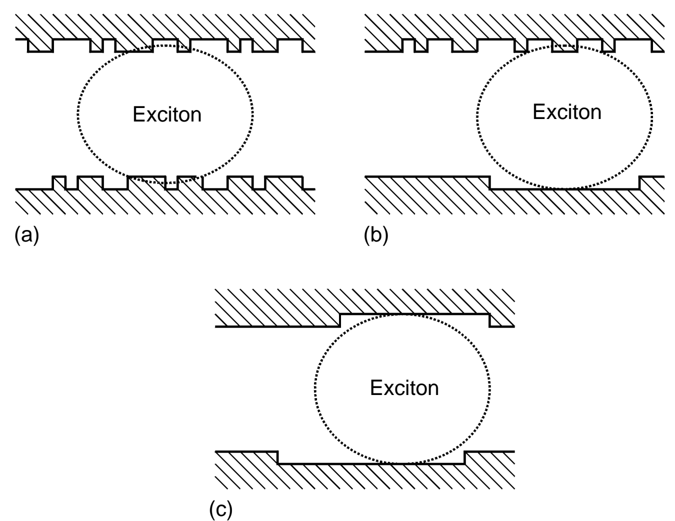


**Figure 10** Models of interface structure relative to the size of the exciton wavefunction: (a) two rough interfaces; (b) one smooth and one rough interface; (c) two smooth interfaces.

than the exciton wavefunction, so the exciton senses a position-dependent distribution of well widths. This phenomenon tends to broaden the PL as excitons recombine in regions with different average well widths. In contrast, when interface island dimensions exceed those of the exciton, most of the recombination occurs within a limited set of QW regions having smooth walls and fixed well width. In this case, discrete lines may be resolved in the QW spectrum.

Because fine structure in low-temperature PL can have many origins, including a variety of impurity transitions, sharp lines in QW spectra must be interpreted with care. Indeed, the growth schedule for the highest quality QWs usually includes growth interruptions at interfaces when excess residual impurities could accumulate. Elman et al. observed splitting in the low-temperature PL of GaAs/AlGaAs QWs, suggesting recombination in well regions differing by one monolayer.[10] However, the lower energy peak (labeled I in Figure 11) vanished with increasing temperature, showing that it was impurity related. Meanwhile, a third peak at slightly higher energy (labeled $E_{HH2}$) gained strength with temperature, identifying it as an intrinsic QW transition. Thermal activation of carriers out of the relatively sparse impurity-related traps quenched the lower energy peak, whereas thermal population of the higher energy intrinsic state raised its PL to a level comparable with that of the lower intrinsic state.

The measured splitting between the intrinsic peaks was found to equal the energy difference expected for wells differing by one monolayer. The PLE spectrum correlates well with the intrinsic states (the impurity state does not appear) and time-resolved spectra demonstrate that they are coupled, confirming the interpretation that the doublet originates in adjacent QW regions with monolayer-thick deviations. Another expected signature of PL multiplets due to QW regions differing by single monolayers is the increased splitting with confinement energy. Deveaud et al. have compiled experimental results demonstrating this phenomenon.[9] This group also uses temperature-dependent PL and PLE to confirm that PL peaks are intrinsic and that excitons created in the narrow regions thermalize to the wider zones.

As described above, observation of PL splitting in QWs is unusual because very smooth interfaces are required. In ordinary QWs, PL broadening is more likely. Because broader lines imply a wider distribution of well widths, narrow PL lines generally indicate high-quality QWs. However, this interpretation can be misleading. Ferguson et al. have conducted an experimental and theoretical study of the effects of a misoriented substrate and growth interruption on the variation in QW line width against well thickness $L$.[28] In samples with uninterrupted growth, the increase in line width with decreasing $L$ corresponded to

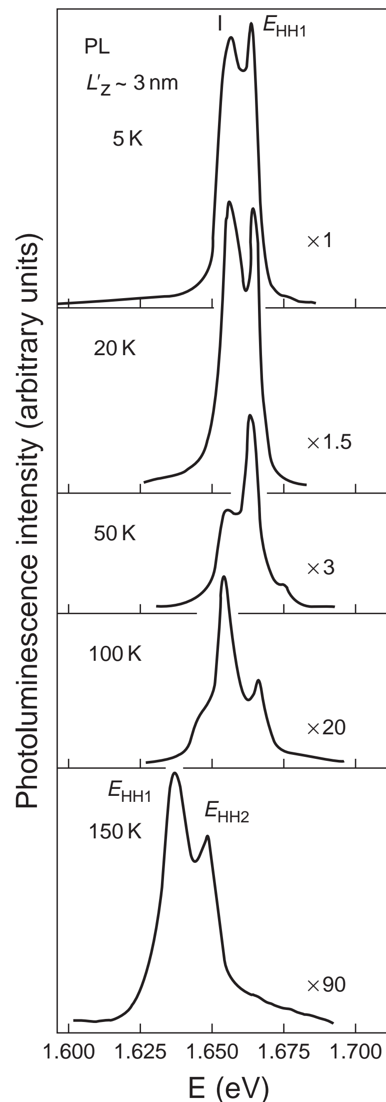


**Figure 11** PL spectra of a GaAs/AlGaAs single QW measured at the temperatures indicated. The peak labeled I disappears with increasing temperature, whereas $E_{HH2}$ rises steadily.[10]

an effective interface roughness of 0.2 monolayers. When growth interruptions are used, the PL line width increased by a factor of 3–4, indicating well-width fluctuations of approximately one monolayer. The increase in line width accompanying growth interruption is attributed to an increase in the lateral extent of interface islands, which is generally regarded as an improvement of the interface. The idea here is that when islands are small the exciton sees a constant average well thickness, but when islands are large the well width depends on exciton position.

In their analysis, Ferguson et al. assumed that the alloy composition of the layers was constant and that the line width reflected interface roughness alone. This interpretation was supported by the strong dependence

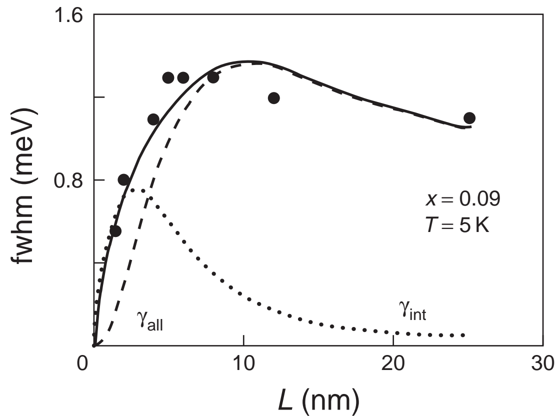


**Figure 12** Experimental (dots) and theoretical (solid line) full width at half-maximum (fwhm) of the exciton recombination line in InGaAs/GaAs QWs. Interface roughness ($\gamma_{int}$, dotted line) and alloy disorder ($\gamma_{all}$, dashed line) contributions to the theoretical result are shown separately.[30]

of line width on $L$. Woods et al. studied the PL of InGaAsP/InGaAsP QWs and came to the opposite conclusion.[29] Because the line width did not increase in the narrow wells, the broadening was attributed to alloy composition variation in the well and barrier layers. In general, of course, both mechanisms will contribute to the PL line width. For example, Patane et al. found that alloy disorder *and* interface roughness are required to fit the $L$ dependence of $In_xGa_{1-x}As/GaAs$ PL lines.[30] Although alloy disorder is sufficient to explain the line width in wide wells, interface roughness is necessary to fit the data at small $L$ (see Figure 12). When $x = 1$, alloy broadening is absent and interface roughness alone must account for the $L$-dependent line width.

## 4 PHOTOLUMINESCENCE INTENSITY

Of all the properties that characterize PL, the intensity of the PL signal has received the most attention in the analysis of interfaces. This interest is due to the fact that, although several important mechanisms affect the PL response, it is generally found that large PL signals correlate with good interface properties. A useful review of the dominant mechanisms and the relationship between them has been provided by Chang et al.[31] In particular, they discuss the roles of the surface recombination velocity $S$ and band bending at the surface in the PL measurement. Because surface recombination is usually nonradiative, and band bending can lead to the formation of a depletion region or "dead layer" where PL is effectively quenched, both of these phenomena tend to reduce the PL intensity. Distinguishing between the two effects is difficult and usually requires a supplementary measurement of the surface potential.

All else being constant, the surface recombination velocity is proportional to the density of surface states. However, changes in the surface-state density can affect the accumulation of charge at the surface, thereby altering the depletion thickness. If increasing the surface-state density enhances the depletion layer, both mechanisms suppress the PL intensity and the surface recombination velocity increases rapidly. Conversely, if the space-charge region is reduced by an increase in the density of surface states, the two mechanisms will have opposite effects on the PL signal and tend to cancel each other out. It should also be noted that, even though changes in surface-state density usually affect band bending, the inverse is not necessarily true. For example, the electric field at the surface can be modified by adsorption of molecules that shift the distribution of electrons between bulk and surface states but leave the surface-state density unchanged. Hence, the coupling of the two phenomena is quite complex.

PL intensity measurements have been used to evaluate a wide variety of surface treatments, including etching, oxidation, hydrogenation, adsorption of gases, deposition of coatings, and heteroepitaxy. The results are usually interpreted within the context of one of the above models: changes in surface-state density or changes in depletion thickness. Occasionally, when supplementary measurements of the surface Fermi level or dependence on applied bias are performed, more sophisticated models that account for both mechanisms are used. Otherwise, restricting the discussion to changes in an effective surface recombination velocity, which contains both effects, can accommodate the ambiguity of the phenomena.

Because a strong PL response is widely regarded as an indicator of a high-quality surface, and PL measurements are nondestructive and environment-insensitive, PL intensity measurements are an important in situ evaluation tool. The PL signal is monitored in real time while the surface is physically or chemically modified. Hence, the advantage of in situ methods is that processing steps can be controlled and optimized precisely. The relative ease of the experiment, combined with the broad implications of results for the optoelectronics industry, has made in situ PL a very popular technique. Indeed, the method has been used to characterize the development of virtually every technologically important surface undergoing almost every technologically relevant process. In these experiments, it is important to bear in mind that PLE itself can induce or accelerate chemical interactions.[32]

As an example, in situ PL has been used to assess InP surfaces during various cleaning and etching steps, oxidation, ambient gas flow, plasma exposure, and

heating.[31,32] In some cases, laser-induced interactions were found to alter etch rates, surface morphology, and surface contamination.[32] The results are explained by the availability of photoexcited electrons and holes that catalyze chemical reactions. In situ PL has also been used to probe the passivation of GaAs with heteroepitaxial AlGaAs monolayer by monolayer.[33] Conducting a similar study outside the growth chamber would have required a long sequence of separate growth runs, where run-to-run scatter in growth conditions could be problematic. Timoshenko et al. have extended the in situ PL technique to evaluate electrochemical treatments of indirect semiconductor surfaces, where pulsed excitation is required to obtain a sufficient PL signal.[34]

An interesting application of surface-adsorbate-induced changes in PL intensity has been described in a series of publications by Ellis et al.[35] Molecular species adsorbed onto semiconductor surfaces can be divided into two categories: Lewis acids that have a large electron affinity, and Lewis bases that have a small electron affinity relative to the work function of the material. Lewis acids draw electrons from the bulk to surface electronic states, and Lewis bases push electrons from surface states into the bulk. These shifts in surface charge expand or contract the depletion thickness of the semiconductor, quenching or enhancing the PL intensity. Hence, the partial pressure of a gaseous species that adsorbs to a semiconductor surface can be inferred by monitoring the PL signal, thus forming the basis for a novel chemical sensor.

### 4.1 Dependence on Applied Bias: Surface Potential

As discussed in section 2.1, the accumulation of charge in low-energy states near the surface leads to curvature of the conduction and valence bands. Representative pictures of this phenomenon are shown in Figure 13. If the surface states trap electrons, negative charge collects at the surface and the bands bend upward. If the surface states tend to lose electrons (trap holes), then positive charge accumulates, curving the bands downward. The electric field associated with this space-charge region sweeps electrons and holes in opposite directions, forming a depletion region free of electrons and holes. Because electrons and holes are spatially separated and cannot recombine, the depleted region is referred to as a dead layer. The PL intensity depends on the thickness of the dead layer, which relies on the magnitude of band bending. Increased curvature extends the recombination-free region deeper into the material, quenching the PL signal.

The magnitude of band curvature is characterized by the surface potential $V_s$ indicated in Figure 13. One can compensate for or accentuate the surface potential $V_s$ by applying an external bias to the surface. The resulting change in the depletion thickness can be evaluated by

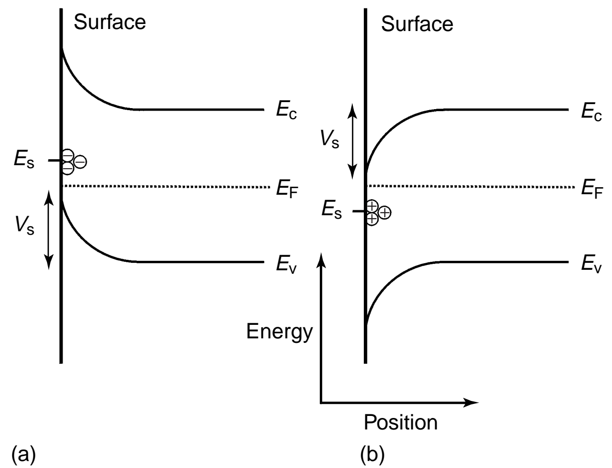


**Figure 13** (a) When electrons accumulate in surface levels (denoted $E_s$), the conduction and valence bands bend upward near the surface. (b) Accumulation of holes bends the bands downward. The magnitude of the effect is characterized by the surface potential $V_s$.

monitoring the PL intensity. Using this approach, surface recombination and band bending contributions to the effective surface recombination velocity can be separated. Indeed, when the external bias exactly cancels the surface potential, the so-called flatband condition is obtained. At flatband, the depletion region is reduced to zero thickness and the intrinsic surface recombination velocity $S_{in}$, excluding dead-layer quenching, can be determined.

For a high-quality surface with a low density of surface states, the dead-layer model alone can explain the dependence of the PL intensity on applied bias. In contrast, when the surface-state density is large, PL quenching is dominated by surface recombination and the dead-layer model does not suffice. Chang et al. have observed both of these scenarios in their study of InP surface treatments.[31] However, they restrict their interpretation to qualitative statements about the relative role of the two mechanisms in PL extinction.

The difference between the bias-dependent PL signal and the dead-layer fit can be used to make a quantitative estimate of the intrinsic surface recombination velocity. Because the dead-layer model assumes that the intrinsic surface recombination velocity is effectively infinite, it underestimates the PL signal for finite $S_{in}$. Kauffman et al. have used this approach to analyze the excitation intensity dependence of the flatband surface trapping velocity at a GaAs/electrolyte interface.[36] The excitation intensity dependence of $S_{in}$ is attributed to the filling of surface states. Hence, the analysis distinguishes between carrier trapping and carrier recombination, which occur at very different rates.

Excitation-dependent shifts in the flatband potential itself have been reported also for the GaAs/electrolyte

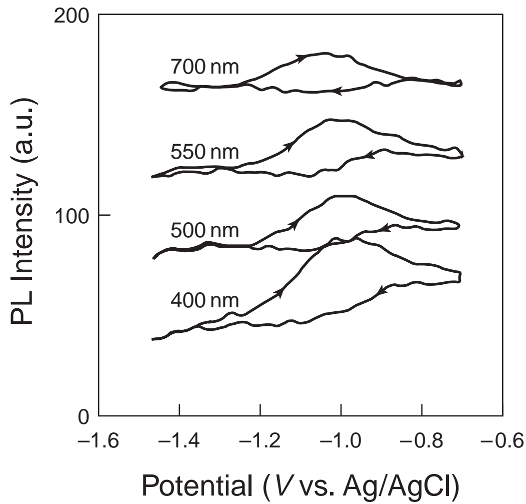


**Figure 14** PL signal at 870 nm vs. applied potential for an etched p-GaAs electrode in 1 M NaOH. Excitation wavelengths are indicated in the plot. The hysteresis in the measurement is attributed to a fundamental change in the nature of the surface during the potential sweep.[5]

interface. Charge and potential distributions at interfaces can be altered dramatically by illumination. One manifestation of the flatband shift is hysteresis in the measurement of PL intensity versus applied bias.[5] It appears that the nature of the surface itself changes under specific biasing and illumination conditions, altering the flatband potential and the associated depletion layer thickness. This phenomenon leads to different bias-dependent PL signals for positive and negative voltage sweeps, as shown in Figure 14.

Under high excitation, surface states are saturated and the accumulation of photogenerated carriers near the surface screens the space-charge field. In this case, a decrease in the PL efficiency reflects the presence of additional surface states. High excitation measurements have been used in this context to study the formation of corrosion-induced surface states at a GaAs/electrolyte interface.[37] After exposure, the PL signal quenches when the applied bias exceeds a value of 1 V above the flatband potential. This result indicates that the applied bias bends the bands and that the new surface states become populated only when the minority carrier quasi-Fermi level reaches the energy of the states. Thus, from the dependence on applied bias, the energetic position of the new levels can be ascertained.

### 4.2 Spatial Dependence: Interface Uniformity and Carrier Diffusion

Because PL intensity is an indicator of interface quality, measurements of the PL signal vs. position provide information on the spatial uniformity of interface properties. The nondestructive and environment-insensitive features of PL make this application particularly useful in the evaluation of substrate surfaces, where detection of electrically active features may help to control problems in epitaxial devices. Such features might be overlooked in mechanical investigations of surface morphology. Although the spatial resolution in a PL scanning application is ultimately dictated by surface area and scan time, the diffraction limit of approximately 1 μm can be achieved in the best experimental arrangements. These high-resolution schemes must address carrier diffusion, which can smear images on a much larger scale.

Spatially resolved PL measurements are usually accomplished by scanning the optical excitation spot relative to the sample surface and detecting the PL signal in the far field. One of the first demonstrations of this approach was made by Krawczyk et al. in an investigation of InP surface treatments.[38] By coupling the excitation into one end of an optical fiber and scanning the other end relative to a focusing objective, they achieved resolution of the order of a few microns. They observed wide variation in the PL signal on a microscopic scale. For example, PL images of the effect of annealing on $NH_4OH$-treated InP are shown in Figure 15. The PL topography evolves from a random distribution of depressions and peaks to a flat response with randomly distributed PL islands. The annealing results are attributed to the presence of small oxide islands that protect the surface from thermal degradation.

Scanning the excitation laser with stepping motors or galvanometer mirrors usually requires a few seconds to accumulate a PL image. However, high-speed rastering with resonant mirrors or acousto-optic devices can generate frames at standard video rates.[39] In this case, PL images can be observed in real time. An additional advantage of video-rate laser scanning is the short dwell time (less than 1 μs) at each excitation position, which minimizes the possibility of photodegradation.

Although spatially resolved PL usually focuses on the band edge or integrated PL signal, spectral selectivity can be incorporated to map the distribution of particular surface states. Tajima has used this approach to plot the deep-level distribution in the near-surface region of GaAs and Si wafers.[40] Because these states tend to saturate at high excitation, he emphasizes the importance of using a low laser power and stabilizing the system mechanically to accommodate long dwell times. He also points out that the surface finish must be controlled carefully to avoid surface-treatment-related phenomena like those discussed above.

The spatial dependence of the PL spectrum itself can be used to evaluate uniformity of alloy composition, epilayer thickness, and a variety of other material properties that affect PL spectra. For example, the PL spectrum has

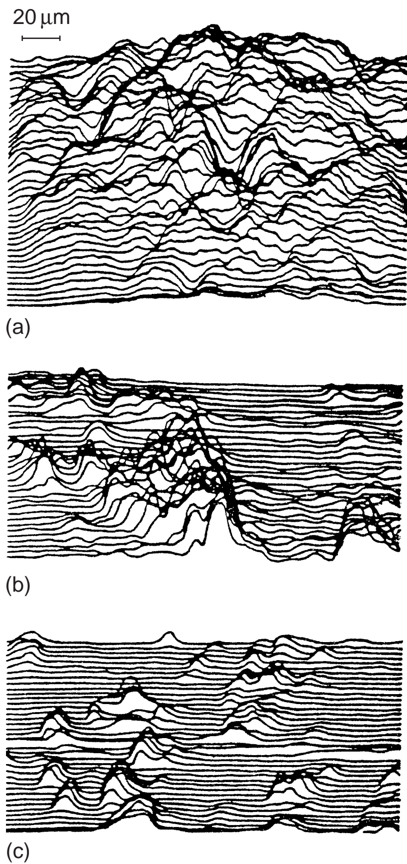


**Figure 15** PL images of InP treated with $NH_4OH$: (a) as treated; (b) annealed at 350 °C; (c) annealed at 450 °C. The PL intensity scale in (b) and (c) is 10 times smaller than in (a).[(38)]

been recorded as a function of position to look for signs of dislocations or residual stress in laterally overgrown InP on InP-coated Si substrates.[(41)] Dislocations are expected to reduce the PL signal, and stress tends to shift and broaden PL peaks. Hence, the spatially resolved InP/Si PL was compared with that of lattice-matched InP layers grown homoepitaxially on InP substrates. The measured PL peak was as strong and narrow as that of the homoepitaxial InP with little shift in peak wavelength, suggesting that the overgrowth layer was dislocation and stress free. In addition, the PL spectrum was independent of position, indicating good uniformity in layer quality.

When a laser is focused on a surface, the minimum spot size is determined by the diffraction limit, which is approximately equivalent to the wavelength of the laser light. In the analysis of semiconductors, the optical excitation energy must exceed the bandgap, which usually corresponds to wavelengths in the visible or near-infrared. Hence, the diffraction-limited spot size is of the order of 1 μm. In the absence of carrier diffusion, the excitation spot size governs the spatial resolution of PL measurements. However, photogenerated carriers often diffuse average distances much larger than 1 μm before recombining, so the PL is generated in a broader region than the original excitation spot. Restricting the PL collection can circumvent diffusion-limited spatial resolution.

The most straightforward approach to this problem is a PL extension of confocal microscopy. Using matched illumination and collection optics with back focal plane apertures, enhanced spatial resolution, improved depth profiling, and insensitivity to scattered light are obtained. Only light originating in the focal spot is imaged by the collection optics. In the context of PL experiments, the configuration rejects luminescence due to recombination of carriers outside the illuminated area. A typical experimental set-up is shown in Figure 16. Fong et al. have used confocal PL to study a GaAs/AlGaAs QW grown on a grooved substrate.[(42)] The improved spatial resolution permitted them to profile abrupt fluctuations (on a scale of 1 μm) in alloy composition and QW thickness. In the confocal measurement, if the detection

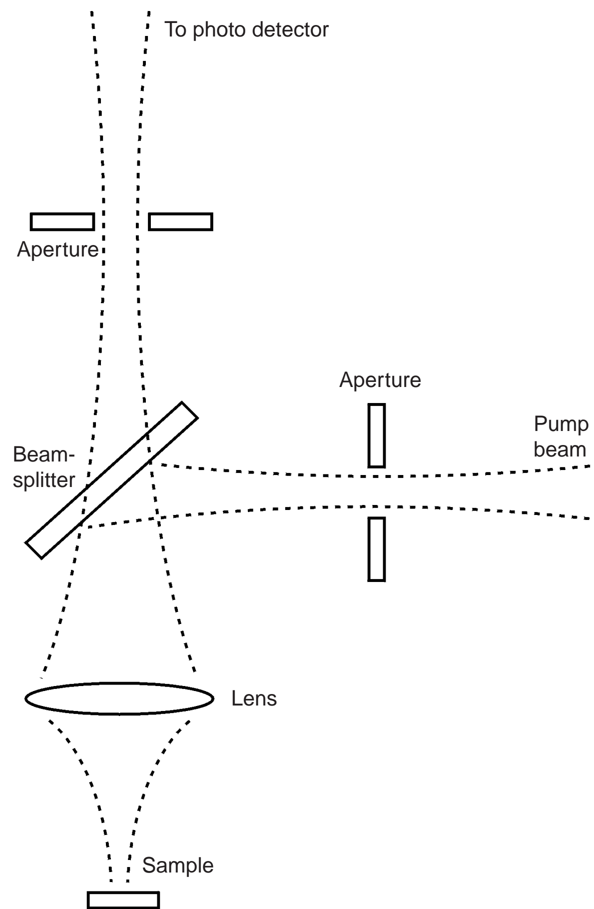


**Figure 16** Typical experimental set-up for confocal PL measurements.

aperture is translated laterally in the image plane, the corresponding detection spot can be maneuvered relative to the excitation spot. This technique can be used to monitor the diffusion process itself. For example, Hubner et al. have measured the diffusion length along semiconductor quantum wire structures.[43] A variation in carrier transport with wire width is explained by changes in sidewall recombination due to different surface-to-volume ratios.

Finally, it should be pointed out that the diffraction limit itself can be surmounted when optical measurements are made in the near-field. If a subwavelength aperture is positioned in the near-field region of the optical emission, resolution comparable to the aperture size can be obtained. The most straightforward manifestation of this idea is to place a mask with a tiny hole very close to the sample surface such that excitation and PL must pass through the aperture. A more popular technique known as near-field scanning optical microscopy utilizes the tip of an extruded optical fiber to excite and/or collect the PL emission. Both of these approaches have produced spatial resolution of the order of 100 nm. Yet, with emission areas this small, generating sufficient PL signal under appropriate excitation conditions can be quite challenging.

### 4.3 Time Dependence: Recombination Rates

When CW excitation is used in a PL experiment, the system quickly converges on steady state. The rate of excitation equals the rate of recombination, and the photogenerated carrier density is constant in time. In contrast, when a material is excited by a series of short laser pulses, the concentration of carriers depends strongly on time. Because the laser pulse can be much shorter than the average recombination time, a specific carrier density can be generated almost instantaneously. The photoexcited carriers then recombine at a rate that is characteristic of the recombination path they follow. Time-resolved PL measurements can be used to determine carrier lifetimes, and to identify and characterize various recombination mechanisms in the material.

Photogenerated carrier lifetimes are obtained by monitoring the transient PL signal after pulsed excitation. Although the experimental apparatus required to make such a measurement depends on the desired resolution, the most common detection scheme is time-correlated single photon counting. When a photon is incident on a photodetector, an electrical pulse is generated. This pulse and an excitation reference pulse are fed into a constant fraction discriminator, which is designed to create output pulses that are timed correctly independent of input pulse size. Next, the signal and reference pulses are sent to a time-to-amplitude converter. This device uses the two input pulses as start and stop triggers for a linearly charged timing capacitor and produces an output pulse whose amplitude is governed by the capacitor charge. Thus, the output pulse height is proportional to the delay between input pulses. The output pulses are sorted according to amplitude and counted by a multichannel analyzer, yielding the transient PL decay.

As discussed in section 2.2, there are three general mechanisms for recombination in semiconductors: SRH transitions via intermediate states, radiative events, and Auger scattering. Equation (1) can be rewritten in terms of the nonequilibrium carrier lifetime $\tau$ as shown in Equation (2):

$$\frac{1}{\tau} = \frac{2S}{d} + \frac{B}{N}n + Cn^2 \qquad (2)$$

It is important to recall that this expression relies on two assumptions: SRH recombination is dominated by interface phenomena and two equivalent interfaces are present in the system. In the analysis of interfaces, we are primarily interested in the SRH term, and in the carrier-density-dependent transition from SRH to bulk recombination. As the excitation level is increased, radiative transitions usually become important well before Auger scattering must be considered. Hence, the Auger term in Equation (2) can be ignored for our purposes. It should be noted, however, that it is possible for low-quality small-bandgap semiconductors with large $C$ coefficients to have Auger rates comparable to the radiative rate when interface recombination begins to saturate.

Neglecting this possibility and assuming that the intrinsic carrier concentration is small, we can identify two important regimes in the carrier kinetics. At low excitation, the carriers are dilute and radiative recombination, which is proportional to $n$, is weak. Hence, the lifetime $\tau \approx d/2S$ is independent of excitation intensity. In this regime, measurements of $\tau$ vs. the active layer thickness $d$ provide direct access to the interface recombination velocity. At the opposite extreme, when interface states are saturated and the radiative rate is fast, $1/\tau \approx (B/N)n$ and the lifetime decreases with increasing excitation. In this context, it is important to realize that $n$ is not constant in time-resolved PL measurements. Rather, it decreases steadily after pulsed excitation via recombination processes. Therefore, at this excitation level one often observes both of the above phenomena in the transient PL signal: fast $n$-dependent decay at early times is followed by a slow, exponential SRH component. Some representative decay curves for GaAs/AlGaAs double heterostructures of varying thickness are shown in Figure 17.[44]

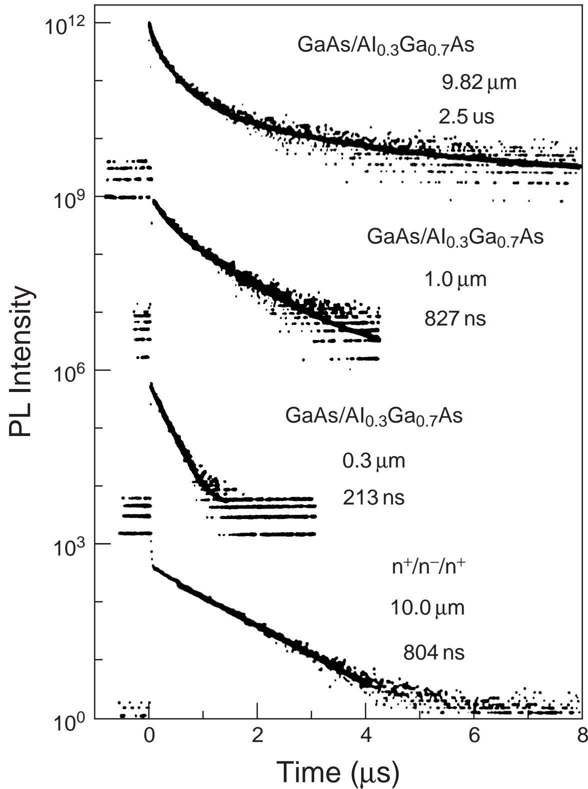


**Figure 17** PL decay curves for a set of GaAs/AlGaAs double heterostructures and an $n^+/n^-/n^+$ GaAs homostructure. Active layer thickness (µm) and carrier lifetime (ns) are indicated in the plot (lifetimes are obtained by fitting the exponential tail of the curves).[44]

Quantitative analysis of such nonexponential multicomponent decay curves is difficult. The situation is simplified in the case of doped materials with relatively high equilibrium carrier concentrations. Here, the photoexcitation can be kept well below the doping level so that the fixed majority carrier density controls the recombination kinetics. Because $n$ is essentially constant throughout the transient measurement, the lifetime is independent of excitation even in the radiative and Auger regimes. Lifetimes in a set of samples covering a wide range of doping concentrations can yield accurate recombination coefficients.[45] In particular, a discrete transition from $n$-independent lifetimes to steadily decreasing $n$-dependent lifetimes should be observed when the carrier concentration reaches the threshold for significant bulk contributions.

Returning to the intrinsic (low equilibrium carrier concentration) case, if the pulsed excitation is kept sufficiently weak then even the initial photoexcited carrier density is within the SRH regime. Thus, an exponential PL decay with a constant lifetime is expected. As described above, the variation in $\tau$ with layer thickness yields

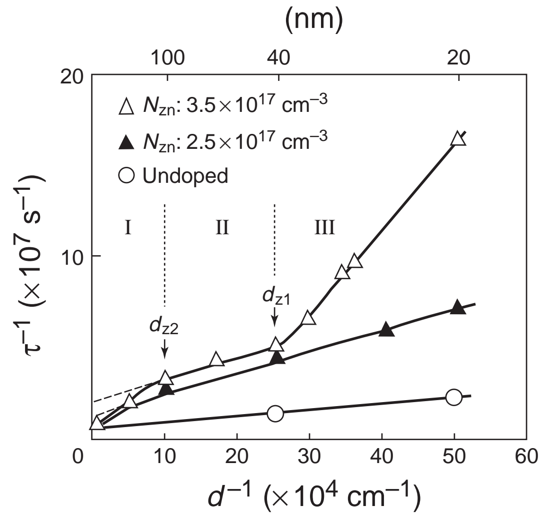


**Figure 18** Recombination rate vs. the reciprocal of the active layer thickness in Zn-doped AlGaInP/GaInP double heterostructures. Symbols representing different doping levels are specified in the plot.[46]

the interface recombination velocity $S$. An excellent example of this type of experiment is the investigation by Domen et al. of Zn doping in AlGaInP/GaInP double heterostructures.[46] Zinc was intentionally incorporated into the upper cladding layer and the resulting carrier lifetime in the active layer was evaluated via time-resolved PL. Measured lifetimes for different doping concentrations are plotted against active layer thickness in Figure 18. The results show the expected behavior ($1/\tau \propto 1/d$) when separated into three regimes that are distinguished by the size of the active layer relative to the Zn-diffused region. In region I, only the top interface is degraded by the presence of Zn. In region II, an increasing fraction of the active layer suffers from diffused Zn. In region III, the high-concentration Zn penetrates all the way through the thin active layer and attacks the bottom cladding interface. The recombination velocities at the relevant interfaces are quickly obtained from the slope of the linear fits.

Time-resolved PL can also be used to distinguish between surface-state and depletion-layer contributions to PL quenching. A decrease in the integrated PL signal implies that the nonradiative recombination rate is enhanced relative to the radiative rate. Such an enhancement can be attributed to one of two mechanisms: an increase in the density of interface states, or an increase in the dead layer thickness. In transient PL, accelerated nonradiative recombination is manifested as a decrease in the photoexcited carrier lifetime. For example, wet-etch surface modification of GaInP has been characterized by CW and time-resolved PL.[47] Etchants yielding enhanced CW PL signals produced corresponding increases in carrier

lifetime, indicating that the nonradiative recombination rate is effectively reduced.

In this particular experiment, it is not clear whether the etching procedure removes nonradiative recombination sites or depletion-inducing surface charge. This shortcoming in the interpretation can be addressed by conducting the transient PL measurements at high excitation, where photoexcited carriers screen the electric field in the space-charge region. If the injection level is sufficiently high, the bands are essentially flat at the surface and changes in the carrier lifetime can be unambiguously attributed to changes in the surface-state density. Lunt et al. have demonstrated this approach in a comprehensive investigation of GaAs surfaces exposed to a variety of sulfur, nitrogen, and oxygen donors.[48] Some treatments produced an increase in the flatband carrier lifetime, indicating a decrease in the intrinsic surface recombination velocity. Meanwhile, other reagents produced substantial increases in the steady-state PL signal but did not affect the high-injection recombination rate. In this case, the results suggest that the enhanced PL is primarily due to changes in the equilibrium band bending. Thus, the two phenomena are effectively separated.

One final application of transient PL to note is the identification of transitions involving type II band alignment. Because these transitions occur between electrons and holes that are separated in real space (see Figure 6), the electron–hole wavefunction overlap is small. Thus, type II optical transitions are expected to proceed more slowly than transitions in type I systems.[19]

### 4.4 Temperature Dependence: Thermal Population

When light is incident on a semiconductor, photoexcitation of electrons from the valence to conduction band can occur for any photon energy exceeding the bandgap. In this process, the difference between the excitation energy and the bandgap goes into the kinetic energy of the photoexcited carriers. Thus, the initial distribution of electron and hole energies depends on energy conservation, not temperature, and the original carrier populations are nonthermal. For example, if the excitation energy is much larger than the bandgap, the electrons and holes will be created high in their respective bands with kinetic energies far exceeding the characteristic thermal energy of the lattice $kT$. The electrons and holes then thermalize with the lattice by emitting phonons and, in the absence of Fermi filling effects, settle into Boltzmann distributions above their respective band edges. Because this process almost always occurs on a timescale much faster than that of recombination, thermal distributions are usually observed in ordinary PL. Thus, in PL experiments, temperature is primarily used to tune the thermal occupation of available states.

At the lowest temperatures, PL is dominated by the lowest energy levels. For instance, excitons (electrons and holes bound by the Coulomb interaction) and shallow impurity traps often appear in low-temperature PL. These states are characterized by binding energies of the order of a few milli-electron-volts, which is small relative to $kT$ at ordinary temperatures. As the sample temperature and corresponding thermal energy are increased, excitons dissociate and carriers vacate shallow traps, reducing the intensity of these features in the PL spectrum. It is important to note here that the PL signal from any level depends on two parameters: the fractional population, and the density of participating states. Thus, relatively sparse low-energy traps appear in low-temperature PL because the thermal population of high-density band levels is very small. However, when the thermal population of band levels is appreciable, band transitions dominate the PL because of the abundance of states taking part.

In addition to the population of discrete states, thermal distributions are manifested in the PL line width of band-edge transitions. When $kT$ exceeds the inhomogeneous broadening in the sample, a high-energy Boltzmann tail appears on the PL peak. This feature can be useful for estimating the local temperature of the sample. However, because thermal quenching can hide sparse low-energy states and thermal broadening can obscure important details in the spectrum, certain PL experiments must be conducted at relatively low (i.e. liquid helium) temperatures.

Relative changes in state population with temperature provide evidence that PL peaks originate in the same part of the sample and that carriers are free to move between the available states. As discussed in section 3.2, multiple peaks in the PL of high-quality QWs are frequently attributed to states in regions of the well differing by single monolayers. In these systems, thermal redistribution among states rules out an important competing explanation: the peaks being due to recombination in separate regions of the sample where carriers do not mix. The temperature-dependent PL spectra in Figure 11 clearly show thermal redistribution among states. The peak labeled $E_{HH2}$ gains strength with increasing temperature, as expected for thermal population of a higher energy state. In contrast, the peak labeled I vanishes at high temperature, demonstrating the importance of the other parameter that controls PL intensity – the density of states. Peak I is strong at low temperature because carriers are trapped at these sites and do not have enough thermal energy to escape, but it disappears at high temperature because the states are sparse relative to the intrinsic bands.

In the characterization of discrete low-energy states, quantitative analysis of the decrease in PL intensity with

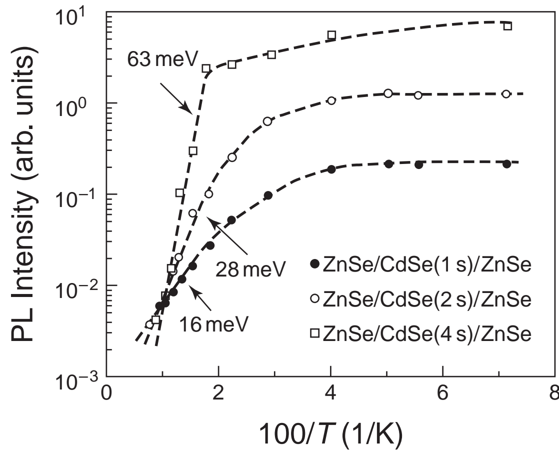


**Figure 19** Arrhenius plots of the temperature-dependent PL intensity from ZnSe/CdSe submonolayer QWs. Deposition times of 1 s, 2 s, and 4 s, as indicated in the plot, correspond to well thicknesses of 1/4, 1/2, and 1 monolayer, respectively.[(49)]

temperature can be used to measure the depth of the trap. Plotting the log of the PL intensity vs. the reciprocal of the temperature, the slope yields the activation energy for exciting carriers out of the traps. These graphs, often referred to as Arrhenius plots, have been used to study interface alloy formation in ZnSe/CdSe QWs.[(49)] Results for three submonolayer wells (1, 1/2, and 1/4 monolayer thick) are displayed in Figure 19. The linear fit at high temperature gives the activation energies shown for delocalization of carriers from the submonolayer well region. When less than one monolayer of CdSe is deposited on ZnSe, two scenarios must be considered. Either distinct CdSe islands form within the ZnSe bulk or atomic interdiffusion leads to ZnCdSe alloying. Here, the increasing well depth with layer thickness indicates that ZnCdSe alloys, not CdSe islands, are formed.

Temperature is also an important parameter in carrier dynamics. The temperature dependence of the carrier lifetime relies on the recombination mechanism and can be used to distinguish between SRH and radiative events. Radiative recombination slows with increasing temperature for two reasons. At the lowest temperatures, excitons dominate radiative transitions and thermal energy in this regime leads to difficulties in momentum conservation. Because photons have small momentum, only low-momentum excitons can directly recombine. Rising temperatures confound recombination by increasing the fraction of excitons with excessive momentum. Beyond this regime, the excitons themselves begin to dissociate and the oscillator strength for free carriers is usually much smaller than that for excitons. In this case, recombining carriers must have equal and opposite momenta, a condition that decreases in likelihood as the average energy increases. In contrast, nonradiative recombination processes tend to accelerate with increasing temperature. In particular, nonradiative interface recombination usually involves thermally activated multiphonon events.[(50)]

A good example of this behavior is the single- and two-photon excitation studies of ZnSe conducted by Wang et al.[(2)] As discussed in section 2.1, single-photon above-gap excitation is absorbed very close to the surface, whereas two-photon excitation penetrates deep into the bulk. In the single-photon excitation experiments, the transient PL reveals short carrier lifetimes that diminish with increasing temperature, as expected for nonradiative surface recombination. In contrast, relatively long lifetimes are observed under two-photon excitation and the lifetime is extended at higher temperatures, indicating that radiative transitions dominate in the bulk.

## 5 PHOTOLUMINESCENCE POLARIZATION

Polarization is another important degree of freedom in optical measurements. In PL experiments, the emission polarization depends on the orientation of the dipole oscillators. Ordinarily, all orientations of electron–hole pair recombination events are equally probable, so the PL is not polarized. However, a variation in PL intensity with electric field orientation is sometimes observed. The maxima and minima in the polarization-angle-dependent PL signal usually occur for electric fields aligned with crystallographic axes. Polarization anisotropy in PL can be attributed to bond asymmetries, alloy composition modulation, and strain.

Investigations of PL polarization in the analysis of interfaces are relatively sparse. Nevertheless, they can be quite useful for identifying qualitative features of interfaces. Vignaud et al. observed large polarization anisotropy in the PL from InAlAs/InP heterostructures.[(19)] They found that the polarization angle yielding the maximum PL signal depended on the specific interface structure. When a thin well of InAs was present at the interface, the PL signal peaked with the polarizer parallel to the [011] axis. On the contrary, when a thin InAlP barrier was present, the PL signal was strongest along [$01\bar{1}$]. Although the exact origin of this phenomenon was not fully understood, the two scenarios agreed with other measurements that distinguished between the two types of interfaces. The polarization anisotropy was tentatively attributed to local interface bond asymmetry.

Another system that has displayed marked PL polarization anisotropy is ZnCdSe/ZnSe QWs grown on GaAs(110) surfaces.[(51)] The variation in PL intensity with polarization angle for one such QW is shown in Figure 20. The ratio of maximum to minimum polarized PL signals can be calculated using Luttinger parameters,

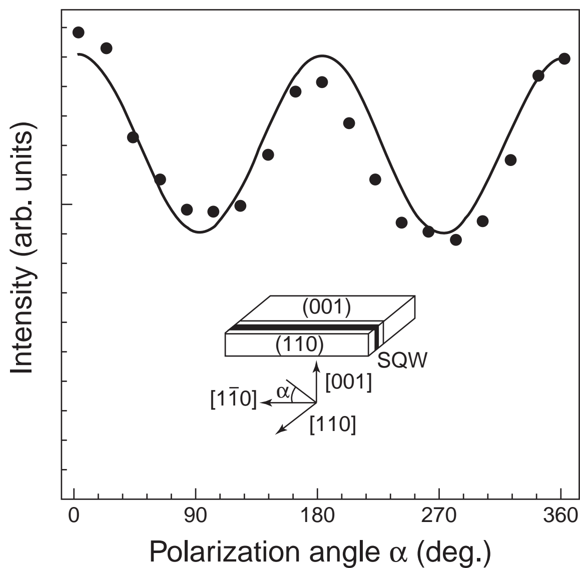


**Figure 20** Polarization angle dependence of the PL intensity from a (110)-oriented ZnCdSe/ZnSe single QW. The solid line is a simple sinusoidal fit.[51]

which describe the valence band dispersion in the semiconductor. Assuming that the Luttinger parameters of ZnCdSe are similar to those of ZnSe, the calculated ratio is much smaller than that found experimentally. The enhanced polarization anisotropy in this system is attributed to compressive strain in the well layer. This interpretation is consistent with the observation of a very narrow PL line width in this sample. Because the lattice mismatch is accommodated by uniform strain rather than dislocations at the interface, the distribution of states in the QW should be relatively sharp.

## 6 CONCLUSION

PL analysis is a powerful tool in the characterization of surfaces and interfaces. Although a number of experimental techniques can provide detailed mechanical information about interfaces, the optoelectronics industry that drives most interface investigations is ultimately concerned with optical and electronic properties. Mechanical information is useful because it is closely correlated with these properties, but PL measurements explore electronic features directly. Other techniques can provide similar access, but they typically require more sophisticated excitation or detection schemes.

PLE is simple, but it is also quite versatile. The excitation energy and optical intensity can be chosen to study different regions and recombination mechanisms near interfaces. Because absorption of the incident light depends on the excitation energy, this parameter determines the depth of the PL probe. Using PLE, absorption and emission energies are observed simultaneously to evaluate the distribution of electronic states. The excitation intensity is even more important, controlling the density of photoexcited electrons. This density is critical in the interpretation of recombination dynamics.

The PL signal itself is characterized by three essential features: energy, intensity, and polarization. Because PL is the result of optical transitions between electronic states, the PL spectrum gives precise information on the energy levels available to electrons in the material. The intensity of the PL signal depends on the rate of radiative and nonradiative events, which depends in turn on the density of nonradiative interface states. Although investigations of PL polarization are still relatively sparse and are not well understood, they can identify unique anisotropic features in the underlying crystal. Future work in this area should lead to a more complete picture of asymmetry at surfaces and interfaces.

PL measurements are not sensitive to the pressure in the sample chamber and can be performed at virtually any temperature. These features make PL an excellent in situ probe of surface or interface modification. Even so, variation of the PL signal with external parameters such as temperature and applied bias can provide additional information on the nature of interfaces. Temperature-dependent thermal activation of electronic states can be used to estimate their depth below the intrinsic bands. An applied bias shifts the bands at the surface, permitting evaluation of the zero-bias band bending. Thus, the availability of PL under a wide variety of experimental conditions provides for advanced measurement opportunities.

Applications of PL analysis range from simple spatial scans of epitaxial wafers to exhaustive investigations of excitation-intensity-dependent PL in novel materials. Furthermore, new PL techniques continue to emerge, expanding the arsenal of PL analysis. Because PLE is usually absorbed near the surface, and interfaces tend to dominate electronic behavior in layered systems, PL is especially well suited to surface and interface investigations. Interfaces are increasingly important in new optoelectronic materials where layered structures are becoming thinner and more complex. Thus, although PL measurements have been useful for the characterization and refinement of such materials, they can be expected to play an even greater role in the future.

## ABBREVIATIONS AND ACRONYMS

| | |
|---|---|
| PL | Photoluminescence |
| PLE | Photoluminescence Excitation |
| $PLS^3$ | Photoluminescence Surface-state Spectroscopy |

QW Quantum Well
RIE Reactive Ion Etching
SRA Spreading Resistance Analysis
SRH Shockley–Read–Hall

## RELATED ARTICLES

*Electronic Absorption and Luminescence* **(Volume 12)**
Surface Measurements using Absorption/Luminescence

## REFERENCES


1. J. Garcia-Garcia, J. Gonzalez-Hernandez, J.G. Mendoza-Alvarez, E.L. Cruz, G. Contreras-Puente, 'Photoluminescence Characterization of the Surface Layer of Chemically Etched CdTe', *J. Appl. Phys.*, **67**, 3810–3814 (1990).
2. H. Wang, K.S. Wong, B.A. Foreman, Z.Y. Yang, G.K.L. Wong, 'One- and Two-photon-excited Time-resolved Photoluminescence Investigations of Bulk and Surface Recombination Dynamics in ZnSe', *J. Appl. Phys.*, **83**, 4773–4776 (1998).
3. R.E. Hollingsworth, J.R. Sites, 'Photoluminescence Dead Layer in p-Type InP', *J. Appl. Phys.*, **53**, 5357–5358 (1982).
4. H. Van Ryswyk, Arthur B. Ellis, 'Optical Coupling of Surface Chemistry. Photoluminescent Properties of a Derivatized Gallium Arsenide Surface Undergoing Redox Chemistry', *J. Am. Chem. Soc.*, **108**, 2454–2455 (1986).
5. K. Uosaki, Y. Shigematsu, S. Kaneko, H. Kita, 'Photoluminescence and Impedance Study of p-GaAs/Electrolyte Interfaces Under Cathodic Bias: Evidence for Flat-band Potential Shift During Illumination and Introduction of High-density Surface States by Pt Treatment', *J. Phys. Chem.*, **93**, 6521–6526 (1989).
6. K. Mettler, 'Photoluminescence as a Tool for the Study of the Electronic Surface Properties of GaAs', *Appl. Phys.*, **12**, 75–82 (1977).
7. Y. Zhu, C. Ding, G. Ma, Z. Du, 'Electronic State Characterization of $TiO_2$ Ultrafine Particles by Luminescence Spectroscopy', *J. Solid State Chem.*, **139**, 124–127 (1998).
8. M. Anpo, M. Kondo, S. Coluccia, C. Louis, M. Che, 'Application of Dynamic Photoluminescence to the Study of Active Surface Sites on Supported Mo/$SiO_2$ Catalysts. Features of Anchored and Impregnated Catalysts', *J. Am. Chem. Soc.*, **111**, 8791–8799 (1989).
9. B. Deveaud, A. Regreny, J.-Y. Emery, A. Chomette, 'Photoluminescence Study of Interface Defects in High-quality GaAs–GaAlAs Superlattices', *J. Appl. Phys.*, **59**, 1633–1640 (1986).
10. B.S. Elman, E.S. Koteles, C. Jagannath, Y.J. Chen, S. Charbonneau, M.L.W. Thewalt, 'Optical Characterization of Single Quantum Wells Fabricated Under Conditions of Interrupted Growth', *Proc. SPIE*, **794**, 44–49 (1987).
11. J.M. Olson, R.K. Ahrenkiel, D.J. Dunlavy, B. Keyes, A.E. Kibbler, 'Ultralow Recombination Velocity at $Ga_{0.5}In_{0.5}P$/GaAs Heterointerfaces', *Appl. Phys. Lett.*, **55**, 1208–1210 (1989).
12. S. Komiya, A. Yamaguchi, I. Umebu, 'Characterization of Radiative Efficiency in Double Heterostructures of InGaAsP/InP by Photoluminescence Intensity Analysis', *Solid State Electron*, **29**, 235–240 (1986).
13. M. Mullenborn, N.M. Haegel, 'Recombination Model for Heterostructure Interfaces', *J. Appl. Phys.*, **74**, 5748–5753 (1993).
14. T.H. Gfroerer, E.A. Cornell, M.W. Wanlass, 'Efficient Directional Spontaneous Emission from an InGaAs/InP Heterostructure with an Integral Parabolic Reflector', *J. Appl. Phys.*, **84**, 5360–5362 (1998).
15. T. Saitoh, H. Iwadate, H. Hasegawa, 'In Situ Surface State Spectroscopy by Photoluminescence and Surface Current Transport for Compound Semiconductors', *Jpn. J. Appl. Phys.*, **30**, 3750–3754 (1991).
16. T. Yoshida, T. Hashizume, H. Hasegawa, 'Characterization of Interface Electronic Properties of Low-temperature Ultrathin Oxides and Oxynitrides Formed on Si(111) Surfaces by Contactless Capacitance–Voltage and Photoluminescence Methods', *Jpn. J. Appl. Phys.*, **36**, 1453–1459 (1997).
17. Y.J. Ding, C.L. Guo, J.B. Khurgin, K.-K. Law, J.L. Merz, 'Characterization of Recombination Processes in Multiple Narrow Asymmetric Coupled Quantum Wells Based on the Dependence of the Photoluminescence on Laser Intensity', *Appl. Phys. Lett.*, **60**, 2051–2053 (1992).
18. Y.J. Ding, D.C. Reynolds, S.J. Lee, J.B. Khurgin, W.S. Rabinovich, D.S. Katzer, 'Evidence for Strong Spatially Localized Band-filling Effects at Interface Islands', *Appl. Phys. Lett.*, **71**, 2581–2583 (1997).
19. D. Vignaud, X. Wallart, F. Mollot, B. Sermage, 'Photoluminescence Study of the Interface in Type II InAlAs–InP Heterostructures', *J. Appl. Phys.*, **84**, 2138–2145 (1998).
20. M.L.W. Thewalt, A.G. Steele, J.E. Huffman, 'Photoluminescence Studies of Ultrahigh-purity Epitaxial Silicon', *Appl. Phys. Lett.*, **49**, 1444–1446 (1986).
21. K. Akimoto, K. Tamamura, J. Ogawa, Y. Mori, C. Kojima, 'Photoluminescence Study of the Interface of a GaAs/ $Al_xGa_{1-x}As$ Heterostructure Grown by Metalorganic Chemical Vapor Deposition', *J. Appl. Phys.*, **63**, 460–464 (1988).
22. A. Henry, B. Monemar, J.L. Lindstrom, T.D. Bestwick, G.S. Oehrlein, 'Photoluminescence Characterization of Plasma Exposed Silicon Surfaces', *J. Appl. Phys.*, **70**, 5597–5603 (1991).

23. M.A. Foad, M. Watt, A.P. Smart, C.M. Sotomayor Torres, C.D.W. Wilkinson, W. Kuhn, H.P. Wagner, S. Bauer, H. Leiderer, W. Gebhardt, 'High-resolution Dry Etching of Zinc Telluride: Characterization of Etched Surfaces by X-ray Photoelectron Spectroscopy, Photoluminescence and Raman Scattering', *Semicond. Sci. Technol.*, **6**, A115–A122 (1991).
24. M.J. Joyce, M. Gal, J. Tann, 'Observation of Interface Defects in Strained InGaAs–GaAs by Photoluminescence Spectroscopy', *J. Appl. Phys.*, **65**, 1377–1379 (1989).
25. L. Xu, X. Huang, H. Huang, H. Chen, J. Xu, K. Chen, 'Surface Modification and Enhancement of Luminescence due to Quantum Effects in Coated CdSe/CuSe Semiconductor Nanocrystals', *Jpn. J. Appl. Phys.*, **37**, 3491–3494 (1998).
26. F.E.G. Guimaraes, B. Elsner, R. Westphalen, B. Spangenberg, H.J. Geelen, P. Balk, K. Heime, 'LP-MOVPE Growth and Optical Characterization of GaInP/GaAs Heterostructures: Interfaces, Quantum Wells, and Quantum Wires', *J. Cryst. Growth*, **124**, 199–206 (1992).
27. M. Mesrine, J. Massies, E. Vanelle, N. Grandjean, C. Deparis, 'Photoluminescence Energy and Interface Chemistry of GaInP/GaAs Quantum Wells', *Appl. Phys. Lett.*, **71**, 3552–3554 (1997).
28. I.T. Ferguson, C.M.S. Torres, T.M. Kerr, 'The Optical Properties of Thin $Al_{0.3}Ga_{0.7}As$–GaAs Quantum Wells on Misoriented Substrates with [110] Terraces. A Study of Interface Roughness Using Photoluminescence', *Semicond. Sci. Technol.*, **7**, 892–899 (1992).
29. L.M. Woods, P. Silvestre, P. Thiagarajan, G.A. Patrizi, G.Y. Robinson, K.M. Jones, M. Al-Jassim, 'Photoluminescence and Interface Abruptness in InGaAsP/InGaAsP Quantum Wells', *J. Electron. Mater*, **23**, 1229–1233 (1994).
30. A. Patane, A. Polimeni, M. Capizzi, F. Martelli, 'Linewidth Analysis of the Photoluminescence of $In_xGa_{1-x}As$/GaAs Quantum Wells ($x = 0.09, 0.18, 1.0$)', *Phys. Rev. B*, **52**, 2784–2788 (1995).
31. R.R. Chang, R. Iyer, D.L. Lile, 'Surface Characterization of InP Using Photoluminescence', *J. Appl. Phys.*, **61**, 1995–2004 (1987).
32. H.J. Frenck, W. Kulisch, R. Kassing, 'Characterization of InP Surfaces Using Integral Photoluminescence Measurements', *Proc. SPIE*, **1144**, 250–258 (1989).
33. C.J. Sandroff, F.S. Turco-Sandroff, L.T. Florez, J.P. Harbison, 'Recombination at GaAs Surfaces and GaAs/AlGaAs Interfaces Probed by In Situ Photoluminescence', *J. Appl. Phys.*, **70**, 3632–3635 (1991).
34. V.Yu. Timoshenko, J. Rappich, Th. Dittrich, 'Express Characterization of Indirect Semiconductor Surfaces by In Situ Photoluminescence During Chemical and Electrochemical Treatments', *Appl. Surf. Sci.*, **123/124**, 111–114 (1998).
35. E.J. Winder, D.E. Moore, D.R. Neu, A.B. Ellis, J.F. Geisz, T.F. Kuech, 'Detection of Ammonia, Phosphine, and Arsine Gases by Reversible Modulation of Cadmium Selenide Photoluminescence Intensity', *J. Cryst. Growth*, **148**, 63–69 (1995), and references therein.
36. J.F. Kauffman, C.S. Liu, M.W. Karl, 'Surface Recombination Kinetics at the GaAs/Electrolyte Interface via Photoluminescence Efficiency Measurements', *J. Phys. Chem. B*, **102**, 6766–6773 (1998).
37. B.A. Balko, G.L. Richmond, 'Corrosion-induced Surface States on n-GaAs as Studied by Photoluminescence Versus Voltage Scans and Luminescence Decays', *J. Phys. Chem.*, **97**, 9002–9008 (1993).
38. S.K. Krawczyk, M. Garrigues, H. Bouredoucen, 'Study of InP Surface Treatments by Scanning Photoluminescence Microscopy', *J. Appl. Phys.*, **60**, 392–395 (1986).
39. G.E. Carver, 'Scanned Photoluminescence with High Spatial Resolution in Semi-insulating GaAs and InP: Aspects of Surface Passivation and Photodegradation', *Semicond. Sci. Technol.*, **7**, A53–A58 (1992).
40. M. Tajima, 'Characterization of Semiconductors by Photoluminescence Mapping at Room Temperature', *J. Cryst. Growth*, **103**, 1–7 (1990).
41. S. Naritsuka, T. Nishinaga, 'Spatially Resolved Photoluminescence of Laterally Overgrown InP on InP-coated Si Substrates', *J. Cryst. Growth*, **174**, 622–629 (1997).
42. Y.-C. Fong, E.A. Armour, S.D. Hersee, S.R.J. Brueck, 'A Confocal Photoluminescence Study of Metalorganic Chemical Vapor Deposition Growth on Patterned GaAs Substrates', *J. Appl. Phys.*, **75**, 3049–3055 (1994).
43. B. Hubner, R. Zengerle, A. Forchel, 'Direct Optical Analysis of Carrier Diffusion in Semiconductor Wire Structures', *Mater. Sci. Eng.*, **B35**, 273–277 (1995).
44. D.J. Wolford, G.D. Gilliland, T.F. Kuech, L.M. Smith, J. Martinsen, J.A. Bradley, C.F. Tsang, R. Venkatasubramanian, S.K. Ghandi, H.P. Hjalmarson, 'Intrinsic Recombination and Interface Characterization in 'Surface-free' GaAs Structures', *J. Vac. Sci. Technol.*, **B9**, 2369–2376 (1991).
45. R.K. Ahrenkiel, R. Ellingson, S. Johnston, M.W. Wanlass, 'Recombination Lifetime of $In_{0.53}Ga_{0.47}As$ as a Function of Doping Density', *Appl. Phys. Lett.*, **72**, 3470–3472 (1998).
46. K. Domen, M. Kondo, T. Tanahashi, 'Analysis for Deterioration of Radiative Efficiency in Zn-doped AlGaInP/GaInP Heterostructures Using Time-resolved Photoluminescence', *Inst. Phys. Conf. Ser.*, **129**, 447–452 (1992).
47. S.S. Kocha, M.W. Peterson, A.J. Nelson, Y. Rosenwaks, D.J. Arent, J.A. Turner, 'Investigation of Chemical Wet-etch Surface Modification of Ga0.5In0.5P Using Photoluminescence, X-ray Photoelectron Spectroscopy, Capacitance Measurements, and Photocurrent–Voltage Curves', *J. Phys. Chem.*, **99**, 744–749 (1995).
48. S.R. Lunt, G.N. Ryba, P.G. Santangelo, N.S. Lewis, 'Chemical Studies of GaAs Surface Recombination Using Sulfides and Thiols', *J. Appl. Phys.*, **70**, 7449–7467 (1991).

49. Z. Zhu, H. Yoshihara, K. Takebayashi, T. Yao, 'Characterization of Alloy Formation at the ZnSe/CdSe Quantum-well Interface by Photoluminescence Spectroscopy', *J. Cryst. Growth*, **138**, 619–624 (1994).
50. L.W. Molenkamp, H.F.J. van't Blik, 'Very Low Interface Recombination Velocity in (Al,Ga)As Heterostructures Grown by Organometallic Vapor-phase Epitaxy', *J. Appl. Phys.*, **64**, 4253–4256 (1988).
51. H.-C. Ko, D.-C. Park, Y. Kawakami, S. Fujita, S. Fujita, 'Fabrication and Optical Properties of ZnCdSe/ZnSe Single Quantum Wells on GaAs(110) Surfaces Cleaved in UHV by Molecular Beam Epitaxy', *Semicond. Sci. Technol.*, **11**, 1873–1877 (1996).